Article

The Lost MIS 11c Mammalian Fauna from Via dell'Impero (Rome, Italy)

Maria Rita Palombo [1,2,*] **, Biagio Giaccio** [1] **, Lorenzo Monaco** [3] **, Roberta Martino** [4,5] **, Marina Amanatidou** [6] **and Luca Pandolfi** [7,*]

1. Istituto di Geologia Ambientale e Geoingegneria, CNR, Area della Ricerca di Roma 1—Strada Provinciale 35d, Montelibretti, 00010 Rome, Italy; biagio.giaccio@cnr.it
2. In Unam Sapientiam Foundation, Sapienza University of Rome, Piazzale Aldo Moro 5, 00185 Rome, Italy
3. Istituto di Scienze Marine, CNR, Via Gobetti, 40129 Bologna, Italy; lorenzo.monaco@cnr.it
4. GEOBIOTEC, Department of Earth Sciences, NOVA School of Science and Technology, Campus da Caparica, 2829-516 Caparica, Portugal; r.martino@campus.fct.unl.pt
5. Museu da Lourinhã, 2530-158 Lourinhã, Portugal
6. School of Geology, Aristotle University of Thessaloniki, 54124 Thessaloniki, Greece; amarinae@geo.auth.gr
7. Dipartimento di Scienze della Terra, Università di Pisa, Via S. Maria, 56126 Pisa, Italy
* Correspondence: mariarita.palombo46@gmail.com or mariarita.palombo@uniroma1.it (M.R.P.); luca.pandolfi1@unipi.it (L.P.)

Abstract: This research presents an in-depth analysis of large mammal remains first discovered in 1932 in the archaeological area of ancient Rome, central Italy, during the work for the opening of Via dell'Impero (VFI). This work describes the faunal assemblage, its current preservation status, and uses tephrochronology to assess its age. Additionally, it provides paleoecological insights into the evolution of the mammalian fauna in Latium, central Italy, from MIS 13 to MIS 7. Analysis of the fossils updates the identification previously proposed by De Angelis d'Ossat, confirming the presence of *Palaeoloxodon antiquus*, *Cervus elaphus*, and *Bos primigenius*. However, in contrast to the previous author, the hippopotamus remains are assigned to *Hippopotamus* cf. *antiquus*, and a second deer is identified as *Dama* sp.. Furthermore, gnawing marks on the hippopotamus femur suggest the presence of a middle-sized carnivore. Tephrochronological investigation was conducted on pumice retrieved from the VFI fossiliferous layer and ash extracted from sediments adhering to the fossil surfaces. The major element composition of the glass from all pumice/ash samples shows a strong affinity with the Vico β unit, allowing correlation with the Fucino record and constraining the deposition of the VFI fossiliferous level between <406.5 ± 1.3 ka and >405.7 + 1.5/−1.6 ka. Radiometric dating is particularly useful for large mammal faunas of MIS 11-MIS 7, a period lacking significant faunal renewals, as Latium mammalian faunas are often dominated by species (elephants, red deer, aurochs) with broad chronological ranges.

Keywords: large mammal fauna; systematics; biometry; biochronology; tephrochronology; MIS 11c

1. Introduction

Precise and accurate chronology for the Quaternary terrestrial vertebrates is crucially needed for understanding their evolution and population dynamics in relation to the specific, regional to continental scale, paleoecological and paleoenvironmental settings and their sensitivity to the rapid and marked cyclical climatic variability that feature this period (e.g., [1–12], and reference therein). Furthermore, well-dated faunal assemblages can be used to assess their spatial and temporal reliability for better disentangling the fauna's evolutionary dynamics in the area. Indeed, solid chronostratigraphic constraints are of crucial relevance for refining biochronological frameworks (e.g., [13–16]).

Unfortunately, the intrinsic nature of the Quaternary sub-aerial terrestrial sedimentary successions containing faunal remains often makes this kind of archive hardly dateable.

This leaves large uncertainties on their age and consequently limits the wealth of the paleontological data for comparisons, from regional to wider geographic scale, and our understanding of the evolutionary processes and population dynamics.

The historical Campagna Romana (Rome Basin, central Italy), which includes the metropolis of Rome and the lower course of the Tiber River valley (Figure 1), arises as a particularly suited area for developing robust, radiometrically based chronologies for the Middle Pleistocene mammalian faunas.
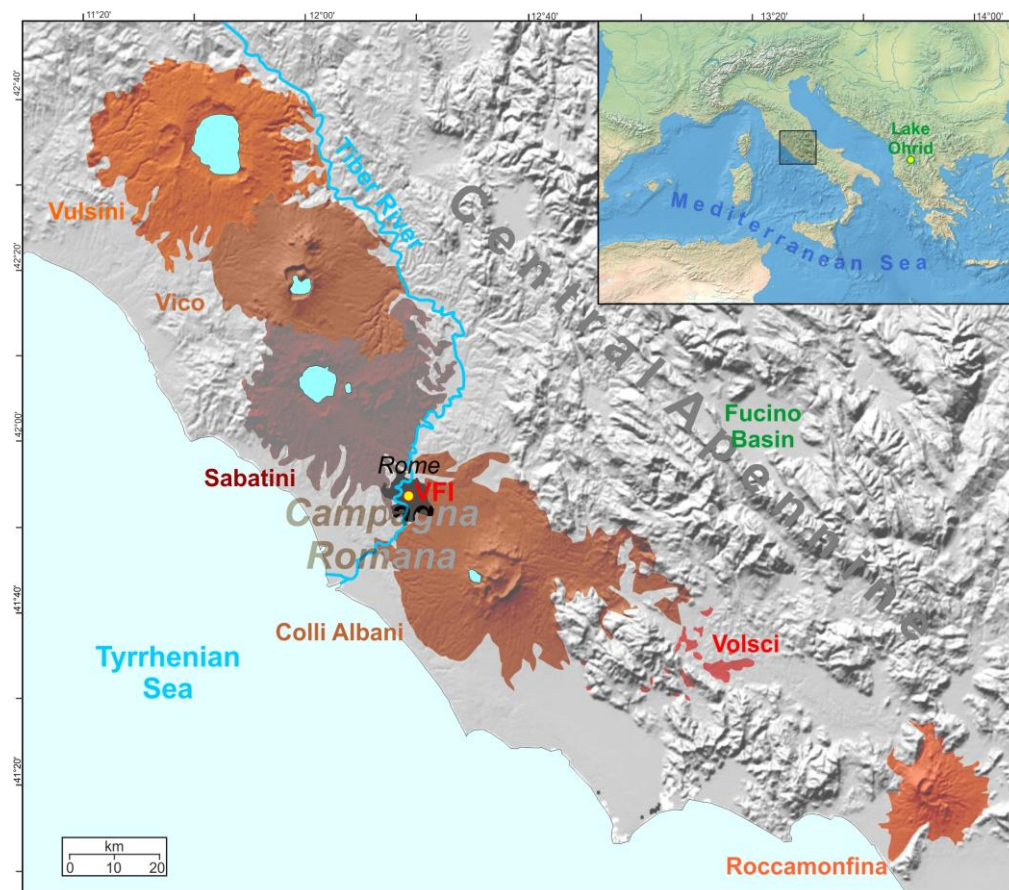

Figure 1. Location of the investigated Via dell'Impero (VFI) faunal assemblage in the city of Rome. The studied locality is characterized by the fluvial-deltaic system of the low course of the Tiber River (Campagna Romana) and of the central Italy peri-Tyrrhenian volcanic system (Vulsini, Vico, Sabatini, Colli Albani, Volsci, and Roccamonfina). The latitude refers to North, the longitude refers to East.

Three crucial factors make this region especially privileged for this purpose: (i) the presence of paleofluvial and paleodeltaic environments, suited for sustaining rich ecosystems with a wide biodiversity, including large populations of mammals; (ii) the close proximity to the peri-Tyrrhenian volcanic system (Figure 1), which was characterized by an ultrapotassic chemism and by intense and continuous Middle Pleistocene explosive activity (e.g., [17] and references therein) that, due to the high content of K-rich minerals, can be precisely dated by ^{40}Ar/^{39}Ar method; (iii) the proximity to the Tyrrhenian Sea (Figure 1), the sea-level glacio-eustatic oscillations, that, combined with the generalized uplift of the Tyrrhenian margin, drove the formation of sedimentary successions, during the progressive phases of progradation to aggradation sea-level rising and highstands (i.e., the glacial termination and the interglacials) and valley incision during sea-level glacial lowstands (e.g., [18–23]). The combination of these factors ultimately results in a series of stacked sedimentary archives related to the main glacial terminations and interglacials of the Middle Pleistocene. Fossiliferous levels containing rich large mammal faunal assemblages (LFAs hereinafter) have been essentially found in transgressive fluvial and fluvio-palustrine

deposits filling incised valleys (TST) and in highstand barrier island–lagoon deposits (HST) (e.g., [24,25]). Most LFAs have been precisely chronologically constrained by means of ^{40}Ar/^{39}Ar dating (e.g., [26,27]), and many others have been correlated with marine isotopic stages and substages based on stratigraphic data.

Nonetheless, no chronological and stratigraphic constraints are available for the historical record of mammalian remains (mainly elephants and hippopotamuses) collected before the first decades of the 20th century from Campagna Romana's deposits and, particularly, from the metropolitan area of Rome. The purpose of this research is twofold: (i) to re-examine the VFI mammal remains that have been recently rediscovered in the Antiquarium Depositorium at Museo della Civiltà Romana (AD-MCR hereinafter), coupled with the description of their current preservation status and the evaluation of their biochronological and paleoecological significance; (2) to provide for the first time a firm chronological constraining via a tephrochronologic approach and, in turn, critically evaluate their implication in the evolutionary context of Latium mammalian fauna and paleoenvironments from MIS 13 to MIS 7.

The Via dell'Impero Within the Frame of Historical Large Mammal Findings in the Rome Subsoil

Huge fossil bones have been reported since the Roman time (cfr. [28]). The drawing "Teschio di Alifante" by the painter Filippo D'Angeli (1589–1629) (alias Filippo Napoletano) depicts a cranium with a mandible which represents the first documented discovery of a fossil elephant in Rome (Figure 2). Several texts, published between the 16th and 18th century, cited the presence of fossils, which were found in the subsoil of Rome, in the *mirabilia* collections of some Roman nobles, providing the first documentation of the discovery of various fossil mammal specimens ([29–31] and references therein).

Figure 2. "Teschio di Alifante" drawing, depicting a skull and mandible that is the first documentation of the discovery of a fossil elephant in Rome (Filippo D'Angeli detto Filippo Napoletano—Teschio di Alifante (Sanguigna—Lille, Musee des Beaux-Art) (Modified after [30]).

A period of widespread urbanization works, which started at the end of the 19th century, led to the exposition of a number of stratigraphic sections and fossiliferous levels and, in turn, to a notable increase in knowledge about the Rome subsoil's geological setting and its vertebrate fossil record. In the 1930s, a new phase of urban structure's reorganization led to a further increase in the paleontological documentation. Among the various findings, the discoveries of the *Homo neanderthalensis* skulls in the Aniene river's gravels cropping

out at Saccopastore (e.g., [32,33]) had the largest resonance. Due to the urbanization that characterizes the Roman area, most of the fossiliferous archives discovered during the past two centuries have been lost or covered due to urban development, and thus are no longer accessible (e.g., [34]). An example of this is, for instance, the Saccopastore site (e.g., [35–37]), along with many other sites that yielded several mammal remains [38]. Among them, one of the most iconic assemblages is that from the so-called "Via dell'Impero" (nowadays, Via dei Fori Imperiali; VFI hereinafter) [39,40] historically represented by a skull of *Palaeoloxodon antiquus* discovered a few hundred meters away from the Colosseum. The discovery of a skull and other elephant remains (Figure 3) took place in 1932 during the works for the opening of VFI, which caused the dismantling of the Velia hill (Figure 4) [41,42].
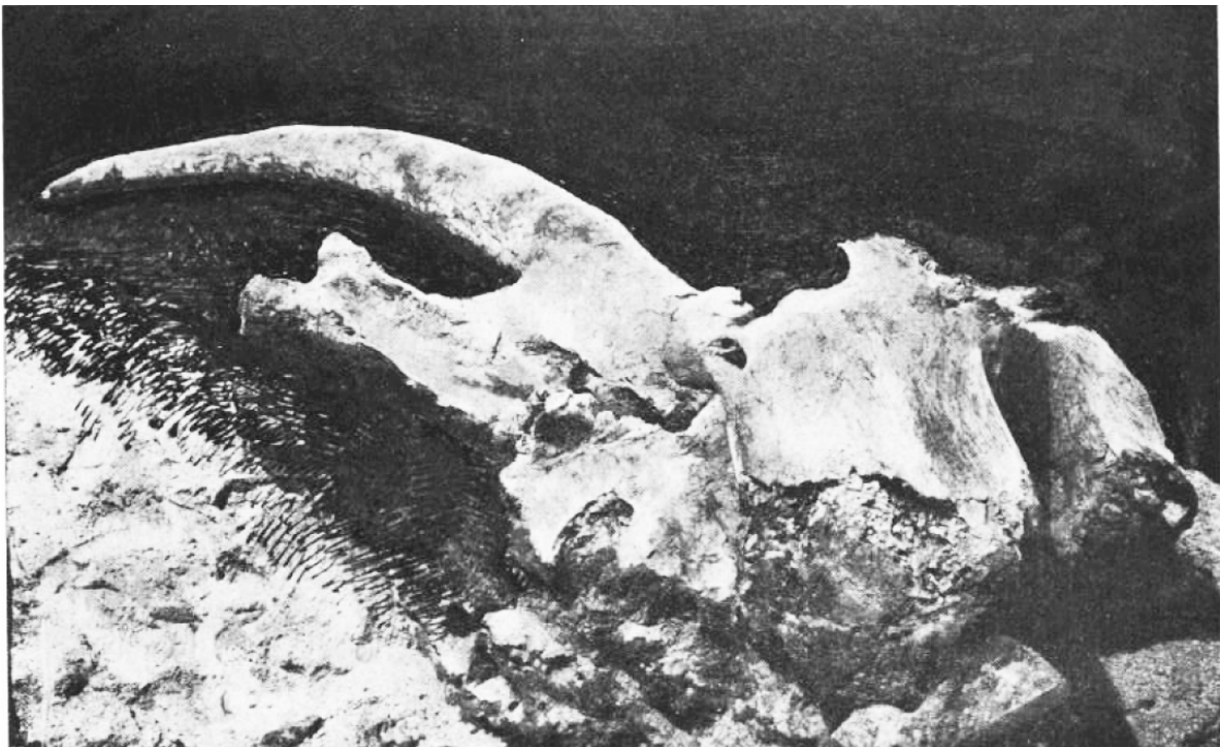

Figure 3. *Palaeoloxodon antiquus*: Picture of the skull found in 1932 during the opening of Via dell'Impero, as it appeared at the time of the discovery (modified after [39], Figure 1).

After their discovery, the *Palaeoloxodon* skull and other mammal remains were quickly recovered to proceed with the construction of the road and subsequently stored at the Celio's Antiquarium. In 1939, the Antiquarium was closed and the VFI archaeological and paleontological material transferred to the Museum of Roman Civilization. Over the following decades, the VFI finds were forgotten, so that the fauna was considered lost. Recently, thanks to the efforts of the Capitoline Cultural Heritage (Sovrintendenza Capitolina), the boxes with the fossil material from VFI were identified. The mammal remains have been partly restored and displayed to the public in 2021 and 2022 during two exhibitions [("La Scienza di Roma", Exposition Palace, and "1932. Il colle perduto", Mercati di Traiano, (McT hereinafter)] [41].

Figure 4. Picture published in media in October 1932, depicting the excavation works for the opening of the VFI and the dismantling of the Velia hill (credit Archive X division Municipality of Rome).

2. Material and Methods

2.1. Material

We studied the mammal remains stored at AD-MCR that belong to different taxa and are mainly fragmented and poorly preserved. The richest mammal sample found in the VFI sandy deposit is represented by the straight-tusked elephant [40]. Currently some specimens are missing, and *P. antiquus* is documented only by a fragmentary skull (AC 49015a) and a partial right tusk (AC 49015b) (both provisionally stored at Mercati di Traiano) [42], a fragmentary mandible (AC 49015d), an isolated upper second molar (AC 49015c), and several undetermined fragments of bones, costae, and vertebrae. The poor preservation of these fragments, which would require a long and invasive restoration, prevents their exhaustive description, and they will eventually be described elsewhere after their restoration.

The family Hippopotamidae is represented by a fragmentary mandible (AC 49636a) divided in at least three main portions ([40] Pl. III, figure c), an isolated first lower incisor (AC 49636a), and a partially preserved femur (AC 49636b) (assigned to Bovidae by De Angelis D'Ossat [40]: Figure 15). The family *Cervidae* is documented by two specimens: a fragment of beam with a tine (AC 49638) ([40]: Figure 14) and a burr with the basal portion of brow tine (AC 49639) ([40]: Figure 13), while Bovidae is represented only by a calcaneus (AC 49637) ([40]: Figure 16). The studied material is impoverished and more fragmented in respect to that described by De Angelis D'Ossat [40], in particular, concerning proboscideans. The postcranial specimens, such as the humerus ([40]: Figure 12), ulna,

and tibia, are missing, as are the two third upper molars belonging to the skull ([40]: Pl. I, figure a). The mandible ([40]: Pl. IIa-b) is currently reduced to some assembled fragmented portions. In the light of that in this work we have described and compared only two third lower molars. A large pumice (AC 49640) ([40]: Figure 4) is also present.

Four samples of sediments were collected from the specimens studied in order to realize some tephrochronological analyses. Among the faunal remains, we sampled between 100 and 200 gr of sediment from the pneumatic cavities of the occipital area of the skull (AC 49015a) and the surface of the right tusk (AC 49015b) of *P. antiquus*, from the right I2 (tusk) pulpar cavity of the *Hippopotamus* mandible (AC 49636a), and from the surface of the large pumice.

2.2. Methods

2.2.1. Measurements and Nomenclature of Mammal Teeth and Bones

For labeling the elephants' chewing teeth, we adopted the nomenclature generally used by the majority of specialists: the first three upper and lower molariform teeth, homologous to deciduous premolar, are named DP2/dp2, DP3/dp3, DP4/dp4, and the three molars M/m1, M/m2, and M/m3. The plates (laminae) present at the mesial (anterior) and distal (posterior) ends of the tooth, which do not extend to the base of the crown, are known as "talons", while we named "platelet" the small lamella that extends to the roots both on the posterior and anterior sides of the molar [43]. Measurements of the molariform tooth were taken following Aguirre [44], Maglio [45], and Lister [46], with minor modifications. For instance, lamellar frequency (F = number of enamel plates in 100 mm in teeth with a total length $\geq$ 100 mm, F* = number of plates in 50 mm in teeth with a length < 10 mm) was estimated averaging the F measured on the occlusal (Foccl), lateral (LFl), and medial (LFm) surfaces to avoid possible mistakes due to the convergence of enamel plates towards the top of the crown, especially in lower molariform teeth.

The description and methodology for the Hippopotamidae remains follow Mazza [47] and Martino and colleagues [38]. *Cervidae* and Bovidae are measured according to Heintz [48] and Driesch [49].

2.2.2. Quantitative Analyses

We briefly examined the VFI large mammal association in the frame of some Latium LFAs, ranging in age from MIS 13 to MIS 7, selected among the best-known LFAs, having some chronological constraints.

We analyze the similarity among the selected LFAs by means of the multivariate classic cluster analysis using the unweighted pair group method with arithmetic mean (UPGMA) algorithm [50], the Q-Mode method, and the metric and symmetrical Jaccard index of similarity. UPGMA and Jaccard index are particularly appropriate for paleontological analyses, basically because in UPGMA, the level at which a member (a case, i.e., a faunal list) joins an existing cluster is based on the average similarity of all the existing members (calculated from the original matrix of coefficients), and Jaccard index is barely influenced by the sample size of the clustering procedure, which was repeated about 10,000 times (bootstrap = 9999).

Statistical cluster analysis was conducted with the PAST (PAleontological STatistics) 4.16 software [51].

Principal component analysis (PCA) on the measurements of lower teeth (L m1, AB m1, PB m1, L m2, AB m2 and PB m2) of different hippopotamus taxa was performed using factoextra, FactoMiner, ggbiplot and ggfortify [52–56] in the RStudio environment [38,57], following the approach used by Martino et al. (2023). Tables with all the measurements used in the analyses are available in the Supplementary Materials (Table S1).

2.2.3. Pumice Analysis

Major and minor element composition of the investigated samples was determined with the electron probe micro analyzer (EPMA). Analysis was performed with a JEOL JXA-

iSP100 Super Probe installed at the Laboratory of Microanalysis and Electron Microscopy (LAM2) of the CNR-IGAG and Earth Science Department of "La Sapienza", University of Rome. The JEOL JXA-iSP100 is equipped with five wavelength dispersive spectrometers (WDS) and one energy dispersive spectrometer (EDS). Analysis was performed at 15 kV accelerating voltage, 10 nA beam current, and 10 μm defocused beam diameter to limit alkali (i.e., Na) mobilization and loss. The following calibration standards have been employed: quartz-NMNH (NMNH = Smithsonian National Museum of Natural History) (Si), ilmenite-NMNH (Ti), anorthoclase-NMNH (Al), olivine (Fe), diopside (Mg, Ca), albite (Na), orthoclase (K), apatite (P), fluorapatite-NMNH (F), sylvite-MUST (MUST = Museo Universitario di Scienze della Terra) (Cl), baryte (S), and metals (Mn). Element counting times on the peak were 10 s (5 s on the background) for Si and Na, 30 s (15 s on the background) for F, Cl, and S, and 20 s (10 s on the background) for all the other elements. Prior to the analytical session, the artificial glass standards of the Max Plank Institute ATHO-G, GOR128-G, and StHs6/80-G [58] were analyzed for quality control. Data reduction and processing was carried out using the ZAF (Z = atomic number; A = absorption; F = fluorescence) correction, while data normalization and visualization was performed in Microsoft Excel®. We adopted 93 wt% as a threshold for the measured total; analyses with total values lower than 93 wt% were discarded. All compositional data are shown as oxide weight percentages (wt%) in the Total Alkali vs. Silica (TAS; [59]) classification diagram and bi-plot diagrams, with total iron (FeOt) expressed as FeO (Fe^{2+}) and normalized to 100% on a volatile-free basis (i.e., excluding F, Cl, and S) for correlation purposes.

3. Results

3.1. Mammal Remains

The skull of *P. antiquus* and the other mammalian remains were discovered at the bottom of Velia Hill's slope, between the Maxentius Basilica and Temple of Venus, in a sandy level rather rich in large pumices. The level was overlaid by a level of earthy tuff and a bank of lithoid tuff ([39,40] Figure 2, p. 7; Figure 5, p. 13). De Angelis D'Ossat [40] provided brief information on the preservation of some fossil remains, mainly elephant specimens, and their distribution in the exposed surface of the sandy level. The incomplete and rather damaged skull was found with its ventral part facing upwards. The premaxillary bones were situated dorsally on the excavation surface, while the well-preserved and almost complete left tusk was still inserted within the alveolus (Figure 3). The mandible, belonging to the same individual, was found close to the skull. Unfortunately, deep fractures separated the mandible into four large fragments and caused the loss of the anterior part of the right molar. However, the horizontal branches were fairly well preserved, and the molars were still in place in their sockets (Figure 5).

At the current state of the art, there is no information in the AD-MCR collection about an isolated, fairly well preserved M2, belonging to a second elephant individual (see below Section 3.1.1) nor about some remains (an atlas, the distal part of a left humerus, the proximal parts of an ulna, and a tibia) that De Angelis D'Ossat [40] briefly described.

At the time of fossil recovery, the tusk was divided into two segments, and the skull was variously damaged, mainly due to the pre-existing fractures. In particular, the anterior portion of the maxillary bone was destroyed, and consequently, the molars separated from the skull. Both molars were recovered and then described by De Angelis D'Ossat [40]. Skull and mandible were further damaged during their transport to the *Antiquarium* and then to AD-MCR (see [42]). The teeth of the skull are not present in the AD-MCR collection and have been presumably lost. Conversely, the hippopotamus, deer, and auroch remains described by De Angelis D'Ossat [40] are nearly all present.

Figure 5. *Palaeoloxodon antiquus*: frontal view of the mandible found in 1932 during the opening of Via dell'Impero, not far from the skull of the same individual (modified after [40], tav. II, figure a).

3.1.1. *Palaeoloxodon antiquus*

- Second upper molar (AC 49015c)

The morphology of the isolated elephant tooth (AC 49015c) clearly indicates that it is an upper first (M1) or second (M2) molar due to its large size, the slightly convex occlusal surface, the large tooth eruption angle, and the almost parallel arrangement of plate, as well as the distal surface worn flat from the pressure of the following tooth. The last character gives to the crown's posterior surface an angulated outline. Moreover, the most posterior plates do not significantly reduce their height as usually happens in the last molar, supporting the attribution of AC 49015c to a M2, (Figures 6 and 7).

The crown of the VFI right M2 is quite well preserved, although broken in three parts that have been perfectly reconnected to each other, whereas the roots are reduced to some entirely missing except for a few small stubs of the most posterior ones. The tooth is rather wide and shows a moderate posterior narrowing, as it more commonly occurs in *P. antiquus*. All the preserved plates are in wear; accordingly, the crown height is not measurable because of the lack of nearly unworn posterior plates ("zone of maximum crown height" in [60]). The first preserved plate is worn to the dentine, though a small segment of the enamel posterior band is still detectable. However, it is hard to distinguish whether the most anterior worn surface should belong to a further plate or to the anterior talon because the crown base and roots are missing. Therefore, we are unable to know the original number of plates. The latter can be estimated if it is possible to identify either the first unpaired root or the inter-root notch that separates the initial root from the subsequent set of paired roots (see [60–62]). Albayrak and Lister [62] noted that in most upper and lower last molars of British *P. antiquus*, two or three plates converge to the first root. The personal observations of one of us (MPR) confirm the latter observation, highlighting the same pattern also for some *P. antiquus* penultimate molars. Since the specimen preserves 11 plates plus the posterior talon, we can reasonably estimate the original number of VFI M2 plates in 13 or more. The size indicates that it is a second molar (Table 1).

Figure 6. *Palaeoloxodon antiquus:* left second upper molar (M2) (AC 49015c) in occlusal view. © Sovrintendenza Capitolina ai Beni Culturali.

Table 1. Tooth measurements of *Palaeoloxodon antiquus* molars from Via dell'Impero (VFI). Abbreviations and symbols: x, talon; p, platelet; ∞, incomplete tooth due to wear or molar break; +, incomplete plate; >, minimum measure of incomplete tooth; -, unable to measure.

Inventory Number		Unknown *	Unknown *	AC 49015c	AC 49015de	AC 49015d
Tooth		M3	M3	M2	m3	m3
Side		Left	Right	Right	Right	Left
Plates	Formula	∞ 15 x	∞ 13.5 x	∞ 11 x	>∞ 15 ∞	+15 ∞
	Total (Pl)	>15	>14	>11	>15	>16
	in use (PlF)	15	13.5	11	14 +	15 +
Length	Total (L)	275	290	239.7	325	
	Occlusal (LF)	250	230	223.1	297.1	300.6
Width	Crown (W)	102	100	ca. 90	ca. 99.9	ca. 101
	Occlusal (WF)	100	100	89.45	87.2	87.5
Crown Height	Crown (H)	-	-	-	-	-
	Functional (HF)	-	-	ca 137	ca 144	-
Lamellar Frequency	Average (F)	6-	5+	5.33	-	4.67
	Occlusal (Fo)	-	-	5	5	5
	Labial (Fl)	-	-	5	-	5
	Buccal (Fb)	-	-	6	4	4
Enamel Thickness	Minimum (em)	-	-	1.71	2.07	1.94
	Average (e)	-	-	2.55	2.79	2.85
	Maximum (emax)	-	-	3.48	3.6	3.8
Hypsodonty index (H/W)		-	-	>1.52	-	-
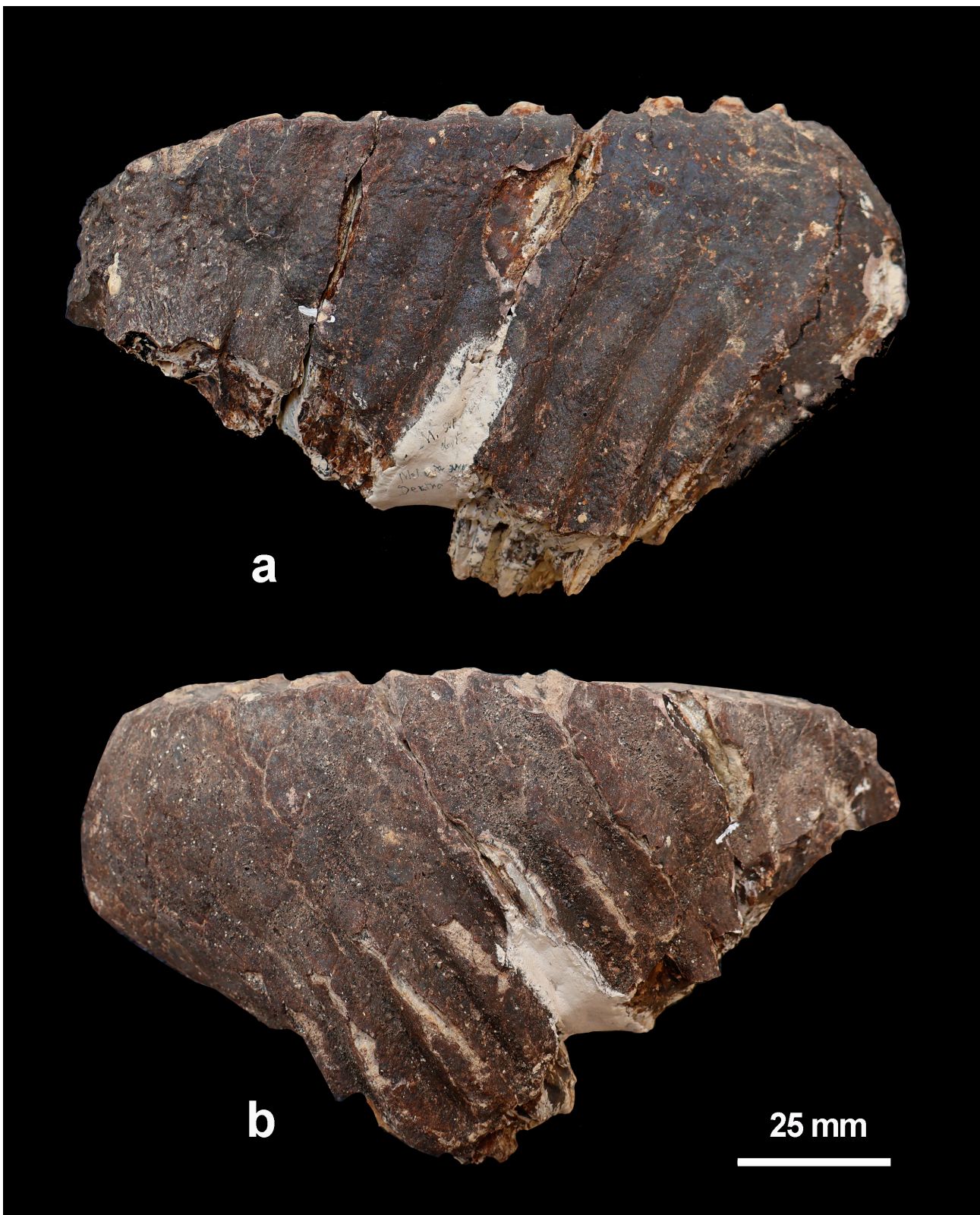
Figure 7. *Palaeoloxodon antiquus:* left second upper molar (M2) (AC 49015c) in buccal (**a**) and labial (**b**) view. © Sovrintendenza Capitolina ai Beni Culturali.

The enamel occlusal figures permit us to easily identify the molar as belonging to *Palaeoloxodon* (Figure 6). Indeed, in terms of occlusal pattern, mammoth and straight-tusked elephant species have distinctly folded enamel and enamel figures. In VFI M2, the enamel

occlusal figures of the plates in early wear show an annular–laminar–annular (dot-dash-dot) pattern, which is particularly evident in the penultimate plate, 10th, and less in the 9th plate that is slightly more worn. The enamel is rather thin, with small folds; a single large medial fold is present on the posterior side of the 9th plate. The central, moderately worn plates are thinly packed; the enamel is irregularly and somewhere coarsely folded with some acute median folds; the 4th, 5th, and 6th plates are slightly curved towards the posterior side and show a moderate expansion along the midline of the tooth, but without giving the figure a 'loxodont' form. These features are not or barely present in *Mammuthus trogontherii*, the only mammoth species recorded in Italy in the Middle Pleistocene, which has more densely packed lamina, thinner enamel, minute folds, and slightly undulate occlusal enamel figures. The latter show a dot-dash-dot pattern in scarcely worn plates and four or more rings in those in early wear. Moreover, the dimensions of VFI M2 fall in the dimensional range of *P. antiquus* specimens, in particular, the Italian ones [63].

VFI M2 shares its morphological features with the third molar of the VFI skull (FO239) that have been depicted and briefly described by De Angelis and D'Ossat [39,40] and described in detail by Palombo and Pandolfi [42] (Figure 8). In VFI M2 and M3, some anterior plates are missing, while all the other plates are in use, though M3 are slightly less worn. Therefore, the penultimate VFI molar does not belong to the skull (FO239) and indicates the presence of a second individual.
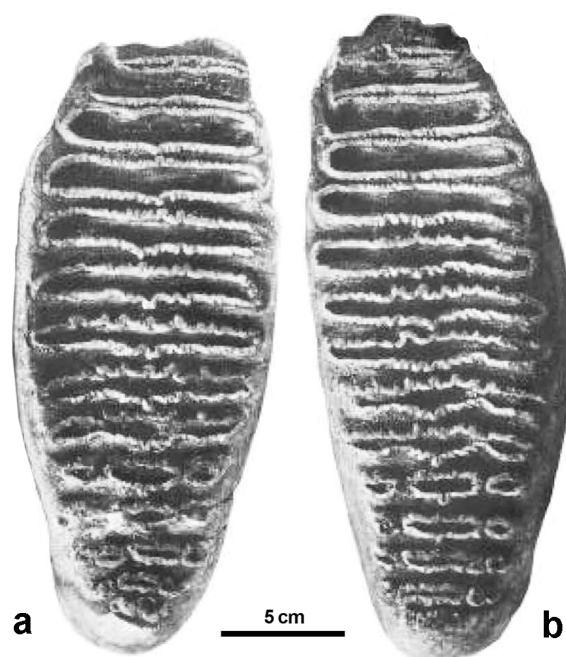

Figure 8. *Palaeoloxodon antiquus:* third right (**a**) and left (**b**) upper molars (M3) in occlusal view. The molars were described by De Angelis D'Ossat [40] but they have been apparently lost (modified after [40], tav. I, figure a).

- Mandible (AC 49015d) and last upper molars (FO238/FO EX 737)

The mandible found in the VFI sandy level not far from the skull was incomplete, lacking the symphysis and the ascending ramus from the coronoid processes to its upper portion. Both molars were inserted in the alveoli. The mandible was fractured and divided into four large fragments (the initial part of the left *ramus mandible*, the left *corpus mandible* broken at the symphysis, and the incomplete right hemimandible, where the anterior half of the mandible corpus was separated from the posterior half, including part of the ascending ramus, by a large fracture) (Figure 5). Unfortunately, during or after its recovery, the mandible was further damaged. The left hemimandible registered the most damage:

the fragment of the left ramus and the anterior part of the right corpus are missing, and the left corpus is broken in the front of the molar.

The wear pattern of last upper molars is close and consistent with the dimensions shown by VFI M3 of the skull (Figures 9–14) (Table 1). The molars, moderately worn, are narrow, curvilinear with the anterior part markedly projected buccally; the enamel is quite thin; folding is rather irregular, with individual folds sometimes angulate and generally not densely packed. In the nearly unworn plates, the enamel occlusal figures are divided in four–five small rings. As the wear increases, the medial rings fuse together, giving the enamel the typical 'dot-dash-dot' form. In the averagely worn plates, large anterior and posterior expansions along the midline of the tooth give the lamella a 'loxodont' form. The medial folds are large, frequently flanked by distinct lateral and medial subsidiary folds. In the plates in advanced wear, the folds' medial expansions are reduced.

5 cm

Figure 9. *Palaeoloxodon antiquus:* left hemimandible large fragment with the third molar (m3) (AC 49015d), in dorsal view. © Sovrintendenza Capitolina ai Beni Culturali.

The left m3 (AC 49015d) is incomplete, since the first plates were lost due to the advanced wear that lowered the plate until the dentine. Only the posterior side of the first plate in use is preserved, the other plates in wear are 14. The molar is almost completely erupted, and the posterior talon is detectable, as it is in the right m3 (Figures 9–11).

In the latter (AC 49015e; Figures 12–14), the first preserved plate is broken at its anterior side. This plate is heavily worn, with the enamel reduced to a small band at the posterior-lateral side. The complete plates in use are 14 plus minute enamel rings belonging to a nearly unworn plate, so that the plates were in total more than 16.

Although the buccal side of the hemimandible is largely broken and most roots are visible, the most anterior part of the alveolus is still present. However, the first root is not detectable, preventing us from inferring the number of lost plates.

Figure 10. *Palaeoloxodon antiquus:* left hemimandible large fragment with the third molar (m3) (AC 49015d), in buccal view. © Sovrintendenza Capitolina ai Beni Culturali.

Remarks

The morphology and dimensions of the skull and its tusk (Palombo and Pandolfi, in press), those of the mandible and of isolated molars, as well as the Schreger lines and angles patterns, perfectly fit with those of *P. antiquus.* The species is one of the most common elements in the Italian LFAS during the Middle and early Late Pleistocene, in particular, from MIS 13 to MIS 5e.

The straight-tusked elephants originated from the African *Palaeoloxodon recki* lineage, whose representatives dispersed out of Africa towards Eurasia in the post-Jaramillo Early Pleistocene. A rather advanced *P. recki* population was present in Israel around 0.8 Ma (MIS 21), as testified by the incomplete skull from Gesher Benot Ya'aqov ([64] and references therein). At that time, the *Palaeoloxodon* dispersal had already taken place, most likely by the end of the Early Pleistocene, maybe triggered by the latest Early Pleistocene cooler and dryer climatic oscillations (MIS 24-22) (cf. [10] for a discussion). The roughly contemporaneous presence of straight-tusked elephants in Turkey at about 0.9 Ma (a last molar from Dursunlu) [64] and in Croatia [the elephant molar ascribed to a new subspecies, *M. meridionalis adriaticus* but likely belonging to *Palaeoloxodon* [61] supports this hypothesis. The molar discovered in the Slivia LFA (northwestern Italy) [65] provides the first reliable evidence of *P. antiquus* presence in Western Europe, presumably shortly before the Matuyama–Bruhnes paleomagnetic reversal, according to the LFA putative age, based on the Slivia small mammal association [66]. In the Middle Pleistocene, straight-tusked elephant remains have been mostly recorded in the South European faunal assemblage. Records of these taxa are rare in central and eastern Europe, where they have mainly been recorded during more recent interglacial phases (from MIS 11 to MIS 7). With the pronounced climatic warming of the last interglacial beginning (MIS 5e), the geographical

range extended northwards as far as the 55° meridian, eastwards possibly as far as the 75° meridian, and southwards till Iran (e.g., [67], and references therein).

Figure 11. *Palaeoloxodon antiquus:* left hemimandible large fragment with the third molar (m3) (AC 49015d), in labial view. © Sovrintendenza Capitolina ai Beni Culturali.

Figure 12. *Palaeoloxodon antiquus:* right lower third molar (m3) (AC 49015e), in occlusal view. © Sovrintendenza Capitolina ai Beni Culturali.

Figure 13. *Palaeoloxodon antiquus:* right lower third molar (m3) (AC 49015e) and a small alveolus fragment in buccal view. The buccal side of the hemimandible is largely broken and some roots are partially visible. © Sovrintendenza Capitolina ai Beni Culturali.
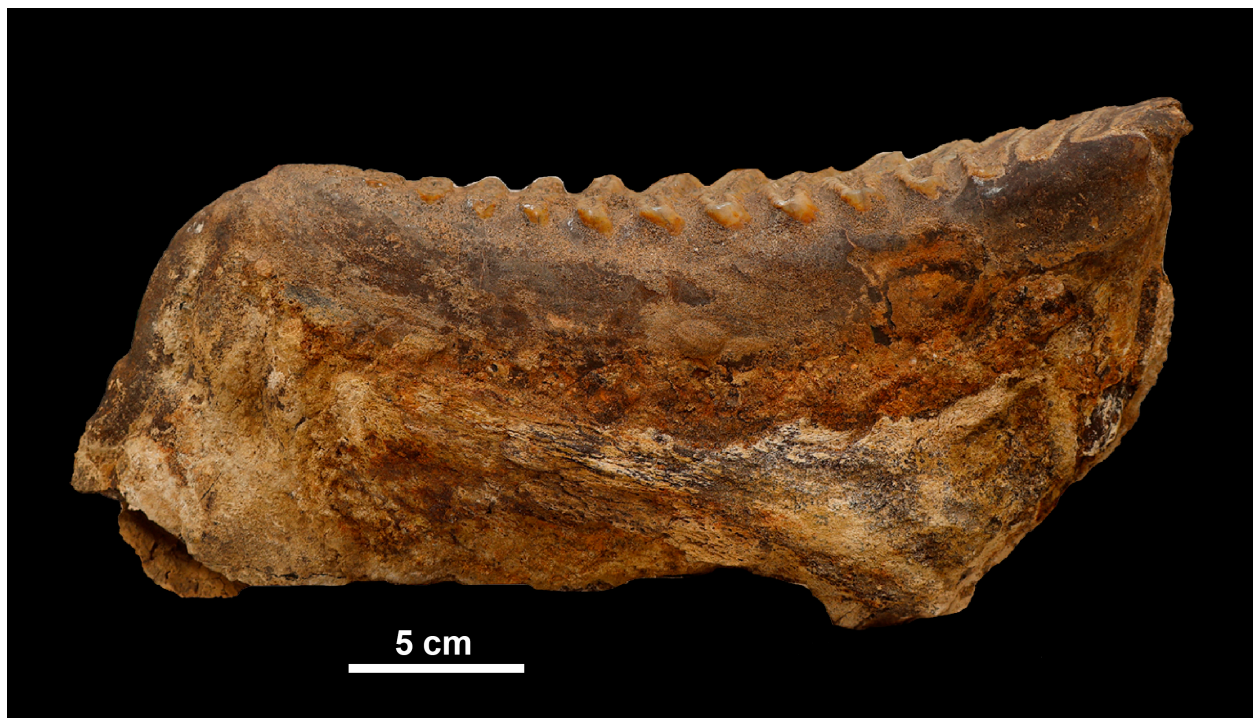
Figure 14. *Palaeoloxodon antiquus:* right lower third molar (m3) (AC 49015e) and a small alveolus fragment in labial view. © Sovrintendenza Capitolina ai Beni Culturali.

The ecological adaptive flexibility of the species accounts for the wide geographic distribution of straight-tusked elephants' populations. *Palaeoloxodon antiquus* inhabited a variety of environments. Indeed, *P. antiquus* remains have been reported from mildly humid environments, warm to warm-temperate areas, and wooded ones, as well as moderately

wooded, and sometimes rather arid, such as grasslands, as documented by the ecological structure of LFAs, pollen, macroflora, and isotopic data (e.g., [68–74]).

Although *P. antiquus* populations survived even during severe Middle Pleistocene glacial phases, they possibly reduced their presence to local suitable environments or shifting their area from central to south Europe. The last glacial-marked climate change (MIS 4-MIS 2) significantly affected the straight-tusked elephant populations, their numerical consistency, and distribution, causing local extinction. By the end of the late last interglacial, in response to the MIS 5a climatic cooling, most populations had gradually reduced their geographic range to core refugial areas, mainly located in southern Europe, particularly in the Iberian Peninsula and in Italy, whereas in Greece, *P. antiquus* has not been reported in the last glacial phase (e.g., [75]). During the late MIS 3 interglacial phase, straight-tusked elephants were still present in the Iberian Peninsula (e.g., in Portugal, an unworn upper molar plate was found, in layers dated to about 33–34 ka at Foz do Enxarrique [76]). The possible occurrence of *P. antiquus* is also reported from Italy, where some remains have been found in the Balzi Rossi, Grimaldi cave, in deposits ranging from MIS 5 to MIS 3 (cfr. [77]), while there is no compelling evidence for the presence of straight-tusked elephants in the Italian peninsula later than MIS 5a to MIS 4 [78]. The extinction of continental populations presumably took place at the transition with MIS 2 since no *P. antiquus* remains have been recorded so far during the Last Glacial Maximum (LGM) (about from 26 ka to 20 ka). Conversely, its insular dwarf descendants were still present during LGM on Favignana (20,350–19,840 cal. BP) [79] and allegedly on Tilos (Greece) until proto-historical times (c. 4 ka, according to [80], but see [81]).

3.1.2. *Hippopotamus*

The hippopotamid material collected from Via dell'Impero is quite scant (Figure 15). The best-preserved specimen is represented by a fragmented mandible, consisting of the rostral fan, with the alveoli of the lower canines, the alveolus of the left lower first incisor, and the section of the right second lower incisor (Figure 15A–F).

The left ramus is also partially preserved, whilst the right one only preserved the alveolus of the second lower premolar. The alveoli of the left premolar series and the first and second lower molars are preserved. The only tooth present is the left third lower molar. The overall aspect of the mandible is rather slender; the rostral fan is not particularly wide, with a small diastema between the first incisors, the first and the second incisors, and between the second incisors and the canines. The first incisors are far larger than the second ones and the cross-section is circular. The second lower incisors are small with a cross-section slightly more elliptical, with the antero-posterior axis bigger than the latero-medial one. The canines are both absent; however, the cross-section of the alveoli is not particularly large, showing a D-cross section. The canine process is robust and rather prominent. The symphysis is short, with a robust cross-section. The left ramus is rather slender in lateral view. The third lower molar is unworn, the metaconid is round, tall, and particularly large, and the protoconid is smaller with a preprotocristid connected to the mesial cingulid. The anterior cuspids do not connect to the posterior ones. The hypoconid is small and mostly circular with a short prehypocristulid, the entoconid is peculiarly small, smaller than the hypoconid and mostly circular. The hypoconulid is still in the alveolus and therefore not investigable. The cingulid is visible in the mesial portion of the tooth, while not investigable in other views. Overall, the not fully erupted third lower molar suggests that the hippo individual was a sub-adult. A right distal fragmented femur is also stored at AD-MCR. The distal articulation is fairly preserved. The trochlea in the anterior view shows clear signs of gnawing. In distal view, the medial condyle is bigger than the lateral one. On the medial portion of the bone the tuberosity for the attachment of ligaments is well visible, as well as the insertion rugosity of the accessory and deep glutei. The condyles are not entirely preserved, and therefore their development is not fully investigable. The intercondyloid fossa is narrow and fairly deep. In *H. antiquus*, usually the rostral fan is less wide than in *H. amphibius*, similarly to the VFI specimen [47]. A less

robust mandible is also usually more common in *H. antiquus*, whilst in *H. amphibius*, the mandible is more robust [47,82–85]. A small diastema between the second lower incisor and the lower canine, similarly to the VFI specimen, is more common in *H. antiquus*, rather than in *H. amphibius* [47]. The unworn third lower molar is not particularly easy to compare with other hippopotamids because they usually show worn-out teeth.
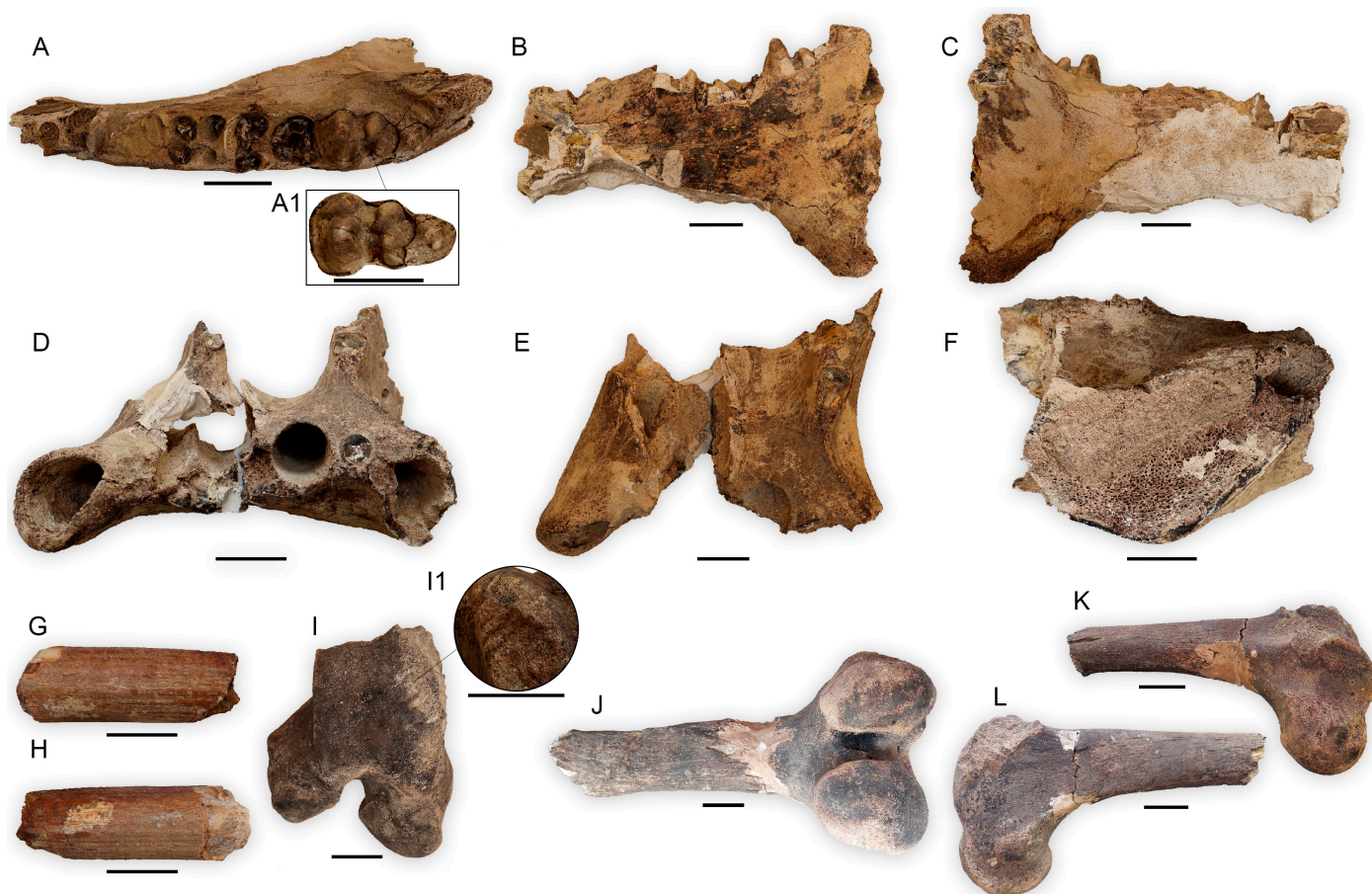

Figure 15. (**A–F**) Fragmentary mandible of *Hippopotamus* (AC 49636a): (**A**) dorsal view of the horizontal ramus, (**A1**) occlusal view of right m3, (**B**) lingual view of the horizontal ramus, (**C**) buccal view of the horizontal ramus, (**D**) anterior view of the incisor corpus, (**E**) dorsal view of the incisor corpus, (**F**) internal view of the symphyseal area; (**G,H**), isolated first lower incisor of *Hippopotamus* (AC 49636a) in (**G**) lateral view, (**H**) anterior view; (**I–L**) partially preserved femur of *Hippopotamus* (AC 49636b) in (**I**) anterior view of the trochlea, (**I1**) gnawing marks above the trochlea, (**J**) posterior view, (**K**) lateral view, (**L**) medial view. Scale bar = 5 cm. © Sovrintendenza Capitolina ai Beni Culturali.

The distal femur shows an intercondylar fossa is slightly inclined, as in *H.* ex gr. *H. antiquus* [47] (Figure 15I–L). In *H. antiquus*, the latter feature is more stressed. Differently from the VFI specimen and the previously mentioned species, *H. amphibius* shows a straighter fossa [47]. The difference in height between the medial and lateral lip, although diagnostic, is not investigable since it is partially missing in the VFI specimen [47]. Morphometrically, the measurements of the LS, Bfi, and Bfo fall within the variability of *H. amphibius* (see Supplementary Materials Table S1). Larger dimensions characterize *Hippopotamus antiquus*. However, the dimensions available of *H. antiquus* are mainly from adult specimens, since juveniles and sub-adults are not really well represented in the fossiliferous record. As demonstrated by Martino et al. [85], the mandible in *H. amphibius*, and most likely in *H. antiquus*, strongly changes during the ontogeny, and therefore sub-adult individuals should have slightly smaller measurements than adults. In addition, the

measurements taken on the mandible are most likely underestimated since the mandible partially misses a part of the symphysis and a part of the bone where the canine erupts. Regarding the teeth, the dimensions are hard to compare since most of them are not preserved (see Supplementary Materials Table S1). However, the measurements of the alveoli of the first and second lower molars are closer to the variability of *H. antiquus* rather than *H. amphibius*. It should be noted that the dimensions were taken on the alveoli and most likely the molars of the VFI specimen were even larger, showing values typical of *H. antiquus*. The anterior breadth of the third lower molar falls within the variability of *H. antiquus*, while *H. amphibius* teeth are usually narrower (Figure 16).
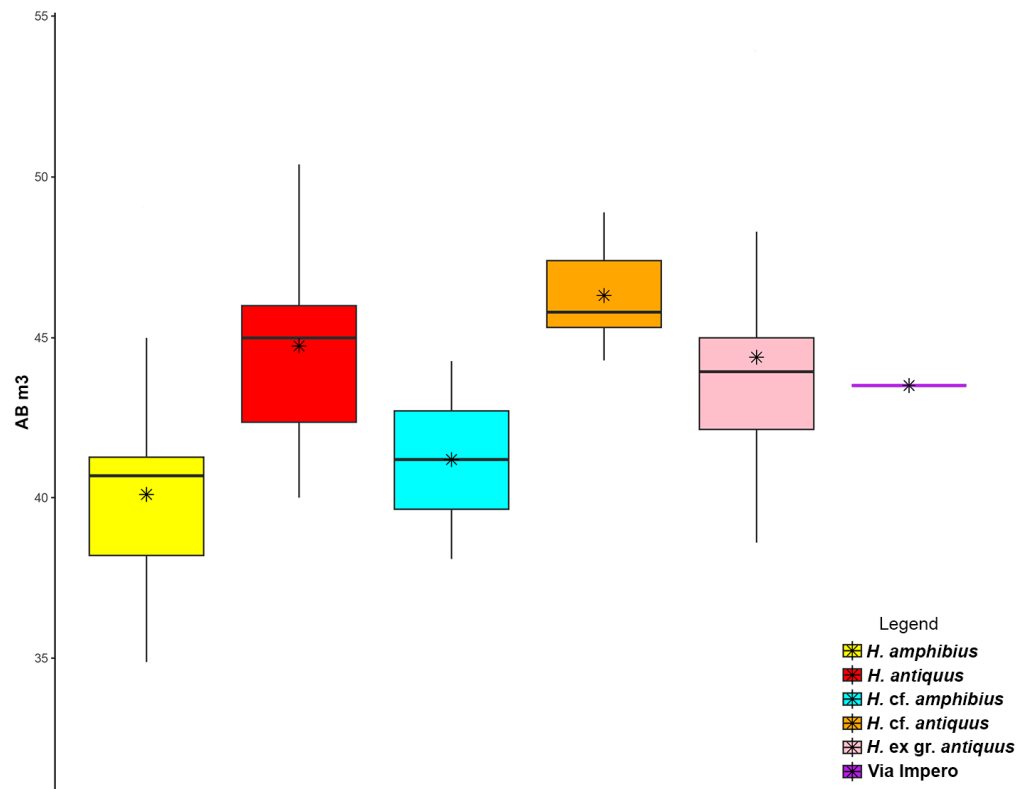

Figure 16. Boxplot of the anterior breadth (AB, in mm) of m3 measurements from different *Hippopotamidae taxa*. For the complete set of measurements, consult Supplementary Materials (Table S1).

Overall, the VFI mandible shows dimensions closer to *H. amphibius*, while the teeth look bigger, being more *H. antiquus*-like. The measurements of the anterior breadth of the third lower molar are close to the *H.* cf. *antiquus* described from Malagrotta, while the second VFI lower molar is peculiarly bigger than in Malagrotta [38]. However, the real measurements of the first and second lower molars could be overestimated or underestimated, since the real teeth are not preserved. The PCA (PC1 62.29% and PC2 16.35%) on the measurements of the teeth (L m1, AB m1, PB m1, L m2, AB m2, and PB m2) show a closer affinity to the *H. antiquus* (see Supplementary Materials, Table S1). The positive values of the PC1 are mostly related to *H. antiquus* specimens, while the negative values characterize *H. amphibius*. The dimensions of the femur (BD 177 mm and DD 220 mm) fall within the variability of *H. antiquus* (Figure 17). The dimensions reported by Mazza [47] for *H. antiquus* (mean BD 196.42 mm, mean DD 226.64 mm) and *H. amphibius* (mean BD 150 mm, mean DD 179.25 mm) also support a closer affinity with *H. antiquus*.
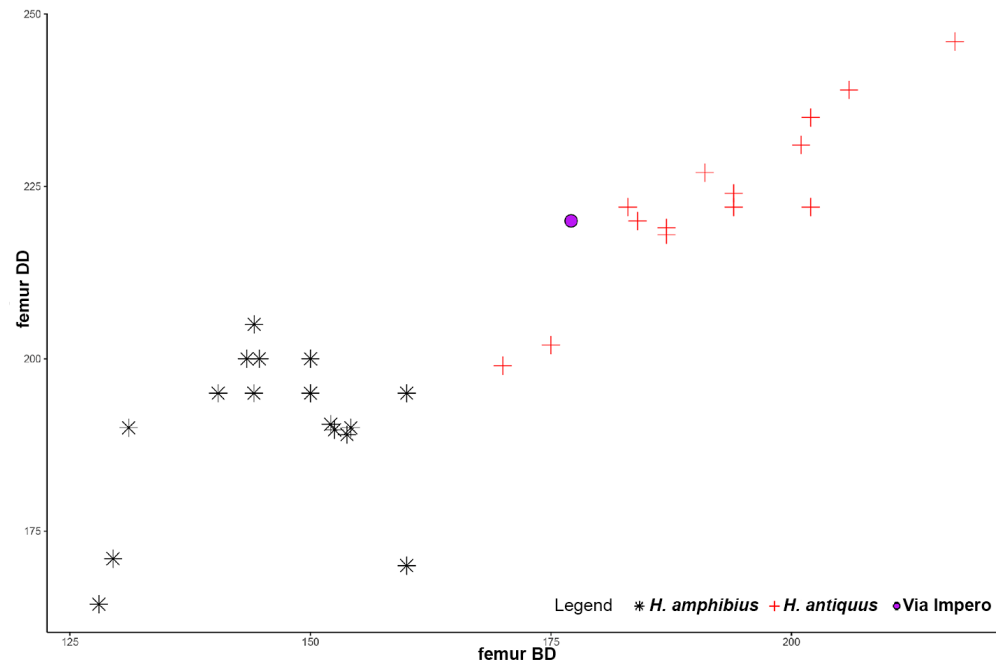
Figure 17. Scatterplot of the femoral distal breadth (BD, in mm) against the femoral distal depth (DD, in mm) from different Hippopotamidae species. For the complete set of measurements, refer to Supplementary Materials (Table S1).

In addition, the presence of either gnawing marks or bite marks on the distal trochlea of the femur suggests the occurrence of a medium-sized carnivore in the VFI assemblage. A small medial portion of the trochlea is missing. In this area, three longer and two smaller marks can be observed. Although these marks are not particularly deep, they are easily recognizable on the bone. The longer marks have a length of around 5 cm, whereas the two smaller ones have a length of 3.41 cm and 1 cm, respectively. The space between each of these marks is around 0.8 cm. Unfortunately, it is not possible to correctly identify which predator made these traces on the hippopotamid femur. However, fossil assemblages of a similar age described in the same geographical area suggest that the possible predator could have been either *Canis lupus*, or *Crocuta* ssp. (See Section 4.4).

Remarks

Although the VFI material is severely fragmented, some characters, such as the small diastema between the first and the second incisor and between the second incisor and the canine, the slender aspect of the corpus, and the small rostral fan, are morphologically closer to *H. antiquus* rather than *H. amphibius* [47,82–85]. The morphometrical analysis on the teeth and on the femur also suggests a closer similarity with *H. antiquus* rather than *H. amphibius*. The comparison of the measurements taken on the mandible is not too reliable since the values have been underestimated. The paucity and the fragmented nature of the VFI specimen do not allow a clear specific attribution. However, the morphology and the morphometry suggest that this hippo was closer to *H. antiquus* rather than *H. amphibius*. In the light of that, the VFI material can be determined as *H.* cf. *antiquus*. The presence of *H.* cf. *antiquus* in the area of Rome around 0.4–0.45 Ma was already demonstrated by Martino et al. [38]. Since the alleged first occurrence datum of *H. amphibius* in Italy has been dated from the same geographical area around 0.5 Ma [86], most likely *H. amphibius* and the last representatives of *H. antiquus* cohabited together before the demise of the large European hippopotamus. The last scenario was already discussed, and, thanks to the hippopotamid material described from VFI, found more credit.

In any case, the presence of hippopotamus within the fossiliferous level strongly supports the presence of stable waterbodies.

3.1.3. *Cervidae*

The family *Cervidae* is represented by a fragment of beam with a tine and a burr with a basal portion of brow tine (Figure 18E–I). The fragment of beam displays a rough surface, longitudinal grooves, and an elliptical cross section (transverse diameter, 37.7 mm; antero-posterior diameter, 44.2 mm). The general features of the specimen suggest an attribution to *Cervus elaphus* rather than to *Dama* or *Capreolus*. The burr is subcircular, and the brow tine is very close to the burr. The surface of the specimen is rather smooth, and the transverse and antero-posterior diameters of the burr are 55.1 mm and 60.57 mm, respectively. The specimen resembles the genus *Dama*, but it is larger than the extant fallow deer. Unfortunately, a firm attribution to *Dama clactoniana* is prevented due to the poorly preserved conditions of the specimen.

Figure 18. (**A–D**) Calcaneus of *Bos primigenius* (AC 49637) in (**A**) anterior view, (**B**) medial view, (**C**) posterior view, (**D**) lateral view; (**E**) partially preserved beam (AC 49638) of *Cervus elaphus* in lateral view; (**F–I**) burr with the basal portion of brow tine (AC 49639) of *Dama* sp. in (**F**) anterior view, (**B**) posterior view, (**H**) internal view, (**I**) external view. Scale bar = 5 cm. © Sovrintendenza Capitolina ai Beni Culturali.

Remarks

The *Cervidae* remains from VFI belong to two different taxa. The fragment of beam is here assigned to the red deer *Cervus elaphus*, and the burr is instead closely related to *Dama*, i.e., *Dama* cfr. *clactoniana*.

Cervus elaphus is a long-lived species in Italy during the Pleistocene, being recorded since the end of the Early Pleistocene. The species is represented by various chronospecies, the validity of which has been discussed by different authors [87]. The red deer is affected by body size changes through the Pleistocene, probably due to climatic fluctuations and population dynamics [88,89]. The occurrence of the genus *Dama* in Italy has been referred to ca. 650 ka by [90] (Vitinia lower gravels). However, Breda and Lister [91] recently suggested a close affinity of these fossil remains with *D. roberti*. *D. clactoniana* occurred in several Middle Pleistocene localities chronologically related with Fontana Ranuccio and Torre in Pietra FUs ([92] but see [93]) (correlated with MIS 11 and MIS 9; [26,94]). Remains of an archaic fallow deer, *D. dama tiberina*, which shows a peculiar mixture of plesiomorphic and

apomorphic features, has thus far been reported mainly from Italian sites and from Grays Thurrock (England; but only considering evolutionary traits of some dental remains: [95]), in particular, from fluvial-lacustrine deposits in the area of Rome chronologically related with MIS 8.5–7 [90,95], whereas the extant subspecies, *D. dama dama*, occurred for the first time at the beginning of the Late Pleistocene [90,95].

3.1.4. *Bos primigenius*

The auroch is only documented by a calcaneus (Figure 18A–D), being the femur reported by De Angelis D'Ossat [40] attributable to *Hippopotamus*.

A bovid is only documented by a calcaneus, being the femur reported by De Angelis D'Ossat [40] attributable to *Hippopotamus*. The specimen belongs to an adult individual and is in good taphonomical condition, showing just some minor breakages on the malleolar articular surface and on the lateral side. It follows the typical Bovini morphology with a robust body and a well-developed tuber calcanei with strong tuberosities. The *sustentaculum tali* is connected to the body through an almost right angle, a character typical of *Bos*. In medial view, the anterior margin of the calcaneal body is straight and flat, and the posterior one has a slight inclination towards the tuber calcanei. The outer margin of the *sustentaculum tali* is curved but does not extend anteriorly on the medial axis, another characteristic of *Bos*. The articular surface for the malleolar is rounded, and the coracoid process is not protruding above it. The articular surface for the astragalus is flat and is mainly D-shaped/semicircular. The distal part of the tali is connected above the cubonavicular facet through an acute angle, creating a V-shaped notch.

The VFI specimen is similar to other *Bos primigenius* calcaneal specimens, such as the ones collected from the early Late Pleistocene of Avetrana, Southern Italy [96]. The latter ones and the VFI specimen are characterized by the attachment of the *sustentaculum tali* to the body through an almost right angle, the lack of the media extension of the *sustentaculum tali*, and the straight and flat anterior and posterior margins. Dimensionally, the studied specimen (H max = 160.58 mm; TD max = 56.56 mm) is definitely smaller than the *Bos primigenius* of Longhua County, China [97] and other European, late Middle Pleistocene and early Late Pleistocene, representatives of *Bos primigenius* (e.g., Avetrana, Grotta Paglicci, Petralona Cave; [98]), and it is close to the minimal values of female individuals from Lunel Viel [99].

Remarks

Bos primigenius represents a common element of the Middle Pleistocene—Holocene fossil faunas of Europe and Asia. *Bos primigenius* occurred early in Italy at Venosa-Notarchirico, ca. 600 ka [100,101], and it was recorded in the fossiliferous localities of the Roman area dated around 500 ka (Valle Giulia Formation, [90]). The early Italian aurochs were smaller and slenderer than those from the late Middle and early Late Pleistocene [96]. The species probably originated from African species belonging to the genus *Bos* (see, [102,103]). This assumption gives rise to various hypotheses concerning a possible parallelism between the diffusion of the *Bos* and the development of the Acheulean culture (Mode II tools) [102–105].

3.2. *Pumice Major Element Composition*

Incipient alteration and diffuse microlites in the glass matrix prevented analysis for the sample labeled MD3-Dx, and limited it for samples Mandible, Tusk-Sx, and skull (1, 3, and 9 analytical datapoints, respectively). Instead, a sufficient number of analytical datapoints, needed to express the full geochemical variability of the volcanic products, was obtained for the sediment samples retrieved from the *Hippopotamus* remains and Pumice (18 and 23 analytical datapoints, respectively).

All samples are characterized by a K_2O/Na_2O alkali ratio >1 (and up to >4) (Figure 19), which can be attributed to the potassic to ultrapotassic magmatism of the peri-Tyrrhenian Quaternary Italian volcanism. In the Total Alkali vs. Silica (TAS; [59]) diagram, the samples plot in the phonolite, trachyte, and rhyolite fields (Figure 19).
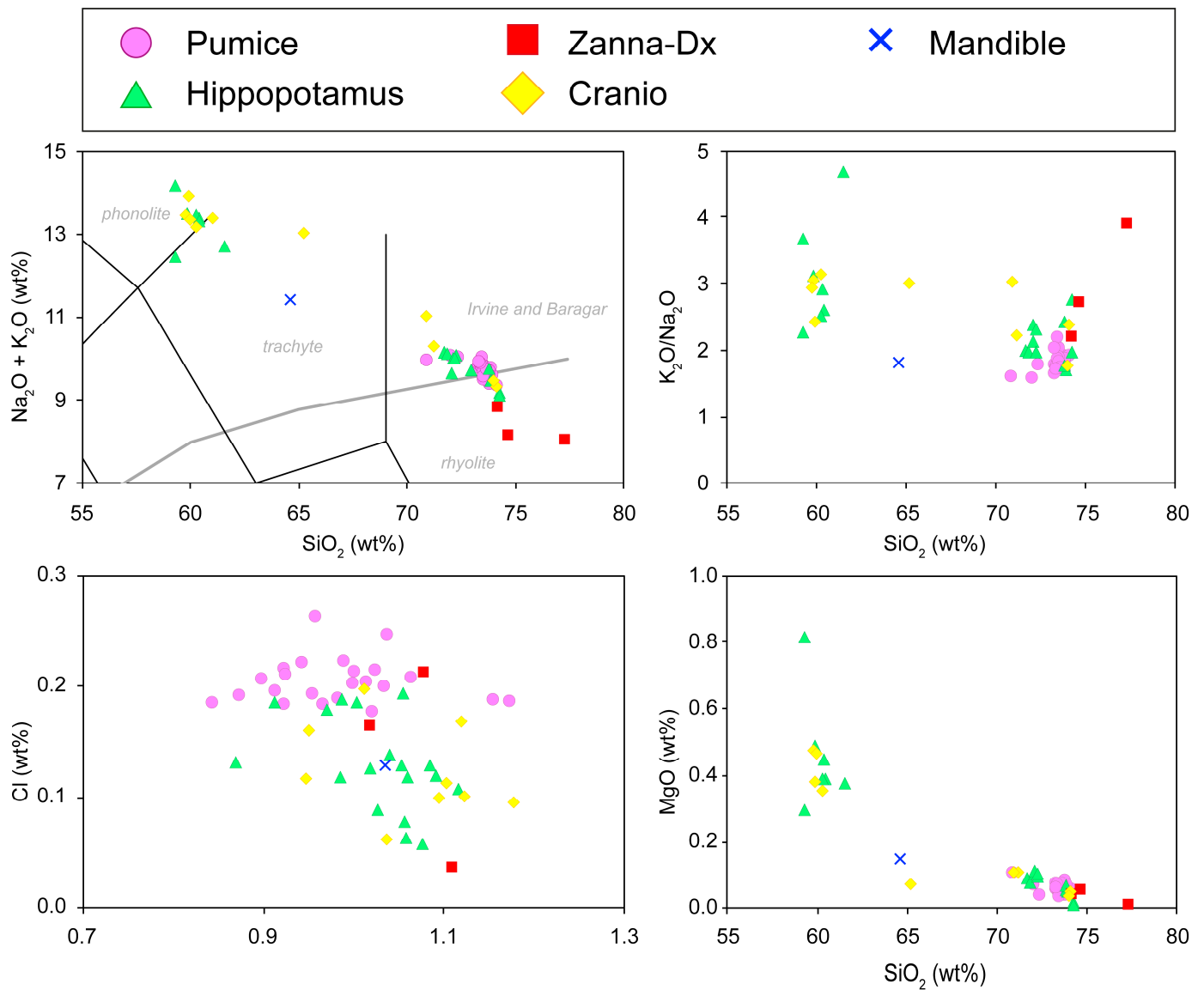
Figure 19. Total alkali vs. silica (TAS; [59]) classification diagram and bi-plot scatter diagrams of the investigated samples.

The pumice sample displays a homogeneous rhyolitic composition, with a mean SiO_2 content of 73.40 ± 1.42 wt% (2 standard deviation), and an alkali sum (i.e., $Na_2O + K_2O$) of 9.74 ± 0.39 wt%. It has an alkali ratio of 1.82 ± 0.28, CaO/FeO ratio of 0.98 ± 0.16, and Cl content of 0.20 ± 0.04 wt%.

The *Hippopotamus* sample has a bi-modal composition, one rhyolitic and one phonolitic-trachytic. The rhyolitic component has a mean SiO_2 content of 72.93 ± 2.10 wt%, a mean alkali sum of 9.73 ± 0.75 wt%, an alkali ratio of 2.13 ± 0.62, CaO/FeO ratio of 1.00 ± 0.13, and Cl content of 0.15 ± 0.06 wt%. Instead, the phonolitic-trachytic component mean composition has a SiO_2 content of 60.15 ± 1.58 wt%, an alkali sum of 13.28 ± 1.12 wt%, an alkali ratio of 3.11 ± 1.66, CaO/FeO ratio of 1.07 ± 0.06, and Cl content of 0.09 ± 0.06 wt%.

Tusk-Sx composition, although represented only by three analytical datapoints, shows a homogeneous rhyolitic composition similar to that of the pumice sample, with a SiO_2 content of 75.40 ± 3.32 wt%, an alkali sum of 8.35 ± 0.84 wt%, an alkali ratio of 2.94 ± 1.75, CaO/FeO ratio of 1.07 ± 0.09, and Cl content of 0.14 ± 0.18 wt%.

The skull sample, like the *Hippopotamus* sample, has a bimodal phonolitic-trachytic and rhyolitic composition. The rhyolitic one has a mean SiO_2 content of 72.55 ± 3.44 wt%, an alkali sum of 10.03 ± 1.57 wt%, an alkali ratio of 2.35 ± 1.04, CaO/FeO ratio of 1.05 ± 0.16,

and Cl content of 0.16 ± 0.07 wt%. The phonolitic-trachytic component instead has a SiO_2 content of 61.03 ± 4.69 wt%, an alkali sum of 13.38 ± 0.69 wt%, an alkali ratio of 2.90 ± 0.55, CaO/FeO ratio of 1.08 ± 0.18, and Cl content of 0.10 ± 0.04 wt%.

Finally, the only analytical datapoint obtained for the mandible sample suggests a trachytic composition, with a SiO_2 content of 64.62 wt%, alkali sum of 11.40 wt%, alkali ratio of 1.81, CaO/FeO ratio of 1.04, and Cl content of 0.13 wt%.

4. Discussion

4.1. The Challenging Task of Chronological Ordering of Latium Late Middle Pleistocene LFAs

Analyzing the evolutionary dynamics of the Pleistocene large mammal fauna on a wider scale is of crucial importance to infer the factors that regulated dispersals, diffusions, and settlements of species in any territory [38]. This, in turn, can be used to determine the taxonomic and structural composition of paleocommunities and mammalian assemblages at local and regional scales. Providing a firm chronological framework of LFAs is hence essential for a more comprehensive understanding of the complex interplay of the underlying causal forces in order to distinguish, for instance, between asynchronous and diachronous dispersal bioevents and to define local versus regional mammal diversity. This will enable us to configure the average fauna structure in a region, such as the Italian peninsula, and its changes over time. It will also allow us to disentangle the factors (e.g., paleoenvironmental s.l., physiographic and geomorphologic, depositional, taphonomic, anthropic, etc.) that might have caused significant disparities in richness, diversity, and structural composition of coeval and geographically close LFAs.

This is in particular the case of the renewal process, started by the end of the Early Pleistocene, that led to the configuration of the late Middle Pleistocene European fauna (the so-called Aurelian fauna) and was completed shortly before MIS 11 [93]. This event marks the beginning of a new climate regime (see below Section 4.3 for additional information). The difficulty in arranging LFAs in a chronological order using only biochronological principles or paleoecological inferences becomes more pronounced when these LFAs, which are poorly diversified and predominantly composed of widely distributed species, inhabited a rather small geographic area characterized by significant physiographic and environmental variations. This applied in particular to the late Middle Pleistocene (MIS 11-MIS 7) LMAs from Latium (Table 2). Moreover, some LFAs belong to historical collections, and therefore most of the mammal remains were collected in localities no longer accessible. Moreover, the stratigraphic data are either unknown or based on old stratigraphic and geochronological knowledge.

Table 2. Chronological ordering of large mammal faunal assemblages (LFAs) from deposits of the lower Aniene Valley, the Roman and Anagni basins, and surrounding area (i.e., Guado San Nicola, and Ciampate del Diavolo/Foresta "Devil's Trails", Caserta), ranging in age from MIS 13 to MIS 7. The selection of the previously mentioned LFAs is justified by their notable historical significance, recent studies or revisions, strong chronostratigraphic constraints, or the inclusion of species that are relevant in terms of chronology or taxonomy. Symbols and abbreviations: ■ = confident presence; ○ = cf. (confer: presence attested by remains with some but insufficient diagnostic characters); ⌘ = presumable identification that has to be confirmed; ✪ = presence inferred on the basis of single badly preserved specimen; **?** = doubtful presence. Green, red, and black colors indicate, respectively, the herein analyzed localities with large mammalian assemblages from Campania, Via dell'Impero (VFI), and southern Latium.

Marine Isotopic Stage	MIS 13				MIS 11								? MIS 11 (? Younger)		MIS 11-MIS 10			MIS 10				MIS 9		MIS 8.5			MIS ? 8.5	MIS 7	
Locality	Casal Selce A	Collina Barbattini and Via Aurelia km 18.9	via Aurelia km 19.3	Cava Rinaldi (upper level)	Via dell'Impero (Via dei Fori Imperiali)	Fontana Ranuccio	Casal Selce B	Casal Lumbroso—Massimina	Castel di Guido	Malagrotta	Riano Flaminio	Via Ostiense Km 2	Cava Panzini-Pontecorvo	Pignataro Interamna	Lademagne (level1-level 2)	Guado San Nicola	Isoletta (ESR1-GA6Z -ESR4)	Cava Pompi	Colle Avarone	Ceprano CG9-CG10	Ciampate del Diavolo	Torre in Pietra 1	La Polledrara di Cecanibbio	Sedia del Diavolo	Prati Fiscali	Monte Sacro	Casal de' Pazzi	Campo del Conte 2	Torre in Pietra 2
Chronology	MIS 13 [106]	MIS 13 [107]	MIS 13 [107]	516 +/− 1 ka [90]	MIS 11c, this work	408 +/− 10 ka [104]	406.5 ± 2.4 ka [108]	MIS 11 c. 400 ka [109]	c. 400 ka [110]	c. 380 ka, MIS 11 [111]	406 ± 5 ka [107]	MIS 11 [112]	? MIS 11–MIS 9	? (various age have been hypotesised, from MIS 11 to MIS 5)	415–381 ka, MIS 11 [113]	409-371 ka–MIS 11 [114,115]	411–346 ka, MIS 11–MIS 10 [113]	<397 +/− 10 ka [113]	? MIS 10 (close in age to CG9-CG10 [116]	>/= 353 ± 8 ka [94,117]	349–350 ± 3 ka [118], MIS 10	MIS 9 [26,119,120]	c. 330, MIS 9 [17,121]	MIS 9 [122,123]; MIS 8.5 (upper level) [107]	MIS 8.5 [107]	MIS 8.5 [107]	MIS 7 [124,125], and upcoming revision	MIS 7 (?) [125]	MIS 7 [26,119,120]

Table 2. *Cont.*

Marine Isotopic Stage	MIS 13				MIS 11								? MIS 11 (? Younger)	MIS 11-MIS 10		MIS 10			MIS 9		MIS 8.5		MIS ? 8.5	MIS 7
Selected Large Mammal Taxa																								
AFROTHERIA																								
Proboscidata																								
Palaeoloxodon antiquus	■	■	■	■	■ (red)	■		■	■	■	■		■	■	■	■	■	■	■	■	■	■	■	■
EUARCHONTOGLIRES																								
Primates																								
Macaca sylvanus sylvanus						■								■							■			■
LAURASIATHERIA																								
Ferae																								
Carnivora-Caniformia																								
Ursidae																								
Ursus deningeri						■																		
Ursus spelaeus				■															○					■
Ursus sp.														■					■				■	■
Hyaenidae																								
Crocuta sp. (*C. intermedia* vel *C. spelaea*).						■											■					■	✪	■
Canidae																								
Vulpes vulpes						○													■		■			■
Canis ex gr. *C. mosbachensis*						■							■											
Canis lupus							■		○								■		■		■	○		■
Canis sp.										■														
Carnivora—Feliformia																								
Felidae																								
Panthera spelaea							■												■					
Panthera pardus																						■		
Panthera sp.						■																		
Ungulata																								
Perissodactyla																								
Equidae																								
Equus sp.																	■	■						
Equus hydruntinus																					■	■	■	■
Equus mosbachensis						■							○		○									
Equus ferus		■						■	■					■		○			■		■	○	○	■
Rhinocerotidae																								
Stephanorhinus hemitoechus			■					■	○									○	■			○	■	■
Stephanorhinus kirchbergensis		○											■		■								■	
Stephanorhinus sp.						■	?								■		■		■				■	■

Table 2. *Cont.*

Marine Isotopic Stage	MIS 13				MIS 11								? MIS 11 (? Younger)		MIS 11-MIS 10			MIS 10				MIS 9		MIS 8.5			MIS ? 8.5	MIS 7
Cetartiodactyla (Artiodactyla)																												
Hippopotamidae																												
Hippopotamus sp.	■	■	■			■				■																		
Hippopotamus antiquus					■				○																			
Hippopotamus amphibius															■	■			○						■	■	■	■
Suidae																												
Sus scrofa						■			?	■			■		■							■	■	■			■	■
Cervidae																												
Capreolus capreolus								✪	■				✪								✪							?
Megacerini gen. et sp. indet						■							■			■		■										
Megaloceros giganteus																		■				■						
C. elephua		■	■	■		■		✪	■	■	■		■	■	■	■	■	■	■	■		■		■	■	■	■	■
Dama sp.		■	■					■							■	■			■									
Dama clactoniana	○	■			⌘	■		○		○	■							○				○		○				
Dama dama ssp.																									■	■	■	■
Bovidae																												
Bos primigenius		■	■	■	■	■		■	■	■			■			■				■		■	■	■			■	■
Bubalus murrensis																							■					

Consequently, the information about the origin and age of pumices and sediments provided by this research is crucial to correctly dating the VFI mammal assemblage, which includes only four species with low biochronological significance. Moreover, the chronological constraint provided by tephrochronology could confirm whether or not the fossiliferous VFI level actually belongs to the fluvial Fosso del Torrino Formation. The last hypothesis was supported by Mancini and colleagues [126], who analyzed the stratigraphic information provided by De Angelis D'Ossat about the Velia and Colle Palatino hills [49,127] in the wider context of the Palatine Hill and surrounding area's stratigraphic framework.

4.2. Origin and Age of the Pumices

In the framework of the Italian Middle Pleistocene explosive volcanism, K-rich rhyolitic glass compositions are extremely uncommon (e.g., [17]). Indeed, hitherto, such silica-high potassium-enriched pyroclasts have been documented only during the early activity of the Vico volcano, and thus this geochemical composition can be regarded as a significant diagnostic feature for tephrochronological purposes [128]. The early activity of the Vico volcano was characterized by the emplacement of two main Plinian pumice fallout deposits, Vico α and Vico β, the latter subdivided in Vico β, *sensu stricto*, and Vico β_{top}, and two other pumice falls from minor explosive events, Vico γ and Vico δ [128,129]. Recently, Pereira et al. [128] provided a rich geochemical dataset (glass major element composition) for all these Vico units and precise $^{40}Ar/^{39}Ar$ dating for Vico α (414.8 $\pm$ 2.2 ka), Vico β (406.5 $\pm$ 2.4 ka), Vico β_{top} (406.4 $\pm$ 2.0 ka), and Vico δ (399.7 $\pm$ 3.2 ka), setting the basis for exploiting their geochemical fingerprinting for tephrochronological purposes.

Despite showing substantial geochemical affinity, using key major elements, especially SiO_2 and Na_2O, the main Vico α and Vico β Plinian units can be reliably distinguished. As a matter of fact, when comparing with the pumice samples extracted from the residual sediment adhering to the surface of the investigated faunal remains, it appears quite evident that the former are more similar to Vico β rather than Vico α (Figure 20), thus allowing attributing the analyzed pumices to Vico β.

In the Roman area, together with Vico α and another reworked Colli Albani-Vico pyroclastic, Vico β forms a series of tephra markers (SPF3, SPF3a, and SPF4 [128]) that are interbedded in Tiber River fluvial-deltaic aggradational sediments formed in response to the sea-level rise during the glacial termination V (TV) and the subsequent MIS 11c sea-level highstand, also called San Paolo Formation (e.g., [130,131]), matching the Torrino Formation [126]. Specifically, the top of the Tiber TV-MIS 11c aggradational succession, or the Torrino Formation, is marked by the volcanoclastic layer SPF4, dated to 403.5 $\pm$ 4.2 ka [128]. Despite the lack of recent direct stratigraphic observations on the nature of the sediments containing the faunal remains, and in particular of the investigated volcanic material, we can assume Vico β, 406.5 $\pm$ 2.4 ka (layer SPF3a), and the layer SPF4, 403.5 $\pm$ 4.2 ka, as *terminus ante quem* and *post quem*, respectively, for the sediment containing the paleontological finds. Summarizing, the large mammal remains can be reliably dated in the narrow temporal span between <406.5 $\pm$ 2.4 ka and >403.5 $\pm$ 4.2 ka, i.e., during the second half of the MIS 11c interglacial (Figure 21).
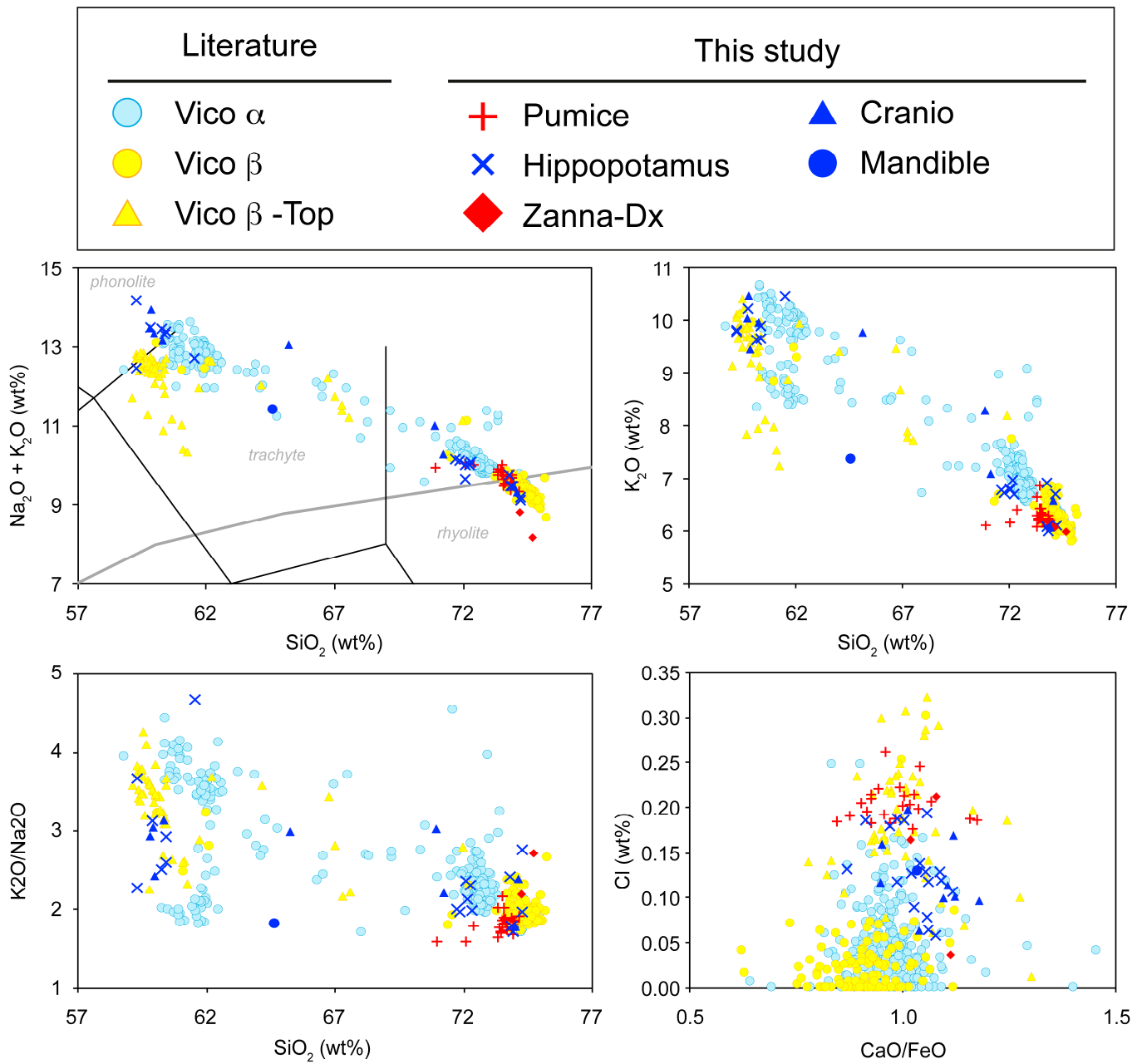
Figure 20. TAS and bi-plot scatter diagrams of the investigated units in comparison with literature data of Vico diagrams of the investigated Plinian fall deposits. Data source: Vico α Plinian fall deposit: [128].

4.3. Chronological, Paleoclimatic-Environmental Setting of the Via dell'Impero Mammal Remains

The MIS 11c (~426–396 ka), the first of the three substages of the MIS 11 (MIS 11c to to MIS 11a, ~426–365 ka), roughly equivalent to the northwestern European Holstenian and British Hoxonian terrestrial interglacials, was the longest and probably warmest Pleistocene interglacial. It was the first interglacial following the Mid-Brunhes event that marked the beginning of an increase in the length and amplitude of glacial/interglacial cycles and could correspond to the end of the Early to Middle Pleistocene Transition [132]. It stands out in Quaternary paleoclimatic history as an anomalous and enigmatic interglacial. The MIS 11c occurred during a relatively weak boreal summer insolation, and its exceptional intensity and long duration (~30 ka), extended for over two processional cycles (e.g., [133,134]).

Due to its peculiar and persistent warm conditions, the MIS 11c climate profoundly influenced both marine and terrestrial ecosystems. In particular, the sea level was 6 to 13 m

higher than present; the atmospheric CO_2 concentration was extraordinary stable and high (265–280 ppm) throughout its entire 30 ka-long duration; the sea surface temperature at high latitudes was warm-temperate; unusual blooms of calcareous plankton were recorded, coral reefs expanded, and the thermohaline circulation intensified (e.g., [135] and references therein). In Europe, as in Italy, a general expansion of forests occurred (e.g., [136,137], and references therein), but with some stadial oscillations and contractions (e.g., [138]), during which winter precipitation and forest cover were lower to those of the Holocene (e.g., [139], and references therein). Recent studies suggested that such peculiar sustained and persisting interglacial conditions of the MIS 11c exerted some influence on the dynamic of the large mammal populations (including those that inhabited the western Latium territory and lived around the Tiber River) by promoting the development of a rich and steady terrestrial ecosystem, which maybe also set the basis for important innovations in the Lower Paleolithic technology [140–147].

Throughout the MIS 11c, as well as through the entire duration of the MIS 11, the ecological structure of most Western Europe mammal fauna was well adapted to the region's mild climatic conditions, and to its expansive forested areas (e.g., [133,148], and references therein). Some climatic stability of the Middle and early Late Pleistocene determined a few species replacements, mainly asynchronous, and scattered moderate renewal of mammalian associations that makes it difficult to chronologically ordering LFAs merely on the basis of biochronological principles. Moreover, new discoveries, the revision of taxa, and new radiometric dating of fossiliferous levels demonstrated that some biologic chronostratigraphic markers (*sensu* [13]), already proposed for the transition from the Galerian to the Aurelian European Land Mammal Ages (ELMAs) [92], appeared during or before MIS 11 ([93], and references therein). For instance, *Canis lupus* has been recorded in the Campagna Romana at Casal Selce-Ponte Galeria (Rome), in a deposit dated at 406.5 ± 2.4 ka, confirming the presence of modern wolf populations in Italy since MIS 11c [102].

In central Italy, detailed MIS 11c records are particularly scarce. The only complete, high-resolution archive close to the site of the faunal finding is that from the Fucino Basin (Figure 1), which also contains the equivalent tephra of the layer SP3, SP3a, and SP4 of the Tiber TV-MIS 11c aggradational unit [149], thus permitting a synchronization of the records (Figure 22). Based on this synchronization, the temporal range of the VFI fossiliferous layer can be further narrowed between <406.5 ± 1.3 ka and >405.7 + 1.5/−1.6 ka, i.e., between the modeled Fucino ages of the tephra TF-116 and TF-108, correlated to Vico β and Centogocce eruptions, respectively (Figure 22).

According to the Fucino XRF Ca record, which is a geochemical proxy of the lake primary productivity [150,151], and thus of the temperature and precipitations, the VFI large mammal remains deposited during a period of rapid environmental–climatic shift, from the relatively warm and humid conditions of the interstadial at ~407.5–405.5 ka to the drier-colder conditions of the first marked stadial of the MIS 11c at 405.5–403.0 ka, of the Fucino Ca record (Figure 22). This rapid and relatively marked transition is also evident in the Lake Ohrid (Figure 1) pollen profile [138], which shows a substantial drop in the temperate trees at ~406.5 ka (Figure 22), when, according to the relative sea-level record of the Red Sea [152], the MIS 11c high-stand peaked at its maximum, to then start declining at ~403 ka (Figure 22). Overall, the regional and extra-regional paleoclimatic records, coupled with the chronological data provided by the pumices analysis, might indicate that the VFI mammals lived during the second half of MIS 11c, which is characterized by more variable and unstable climatic–environmental conditions, compared with the relatively steady warm-humid ones, featuring the first half of this anomalous long and intense interglacial.
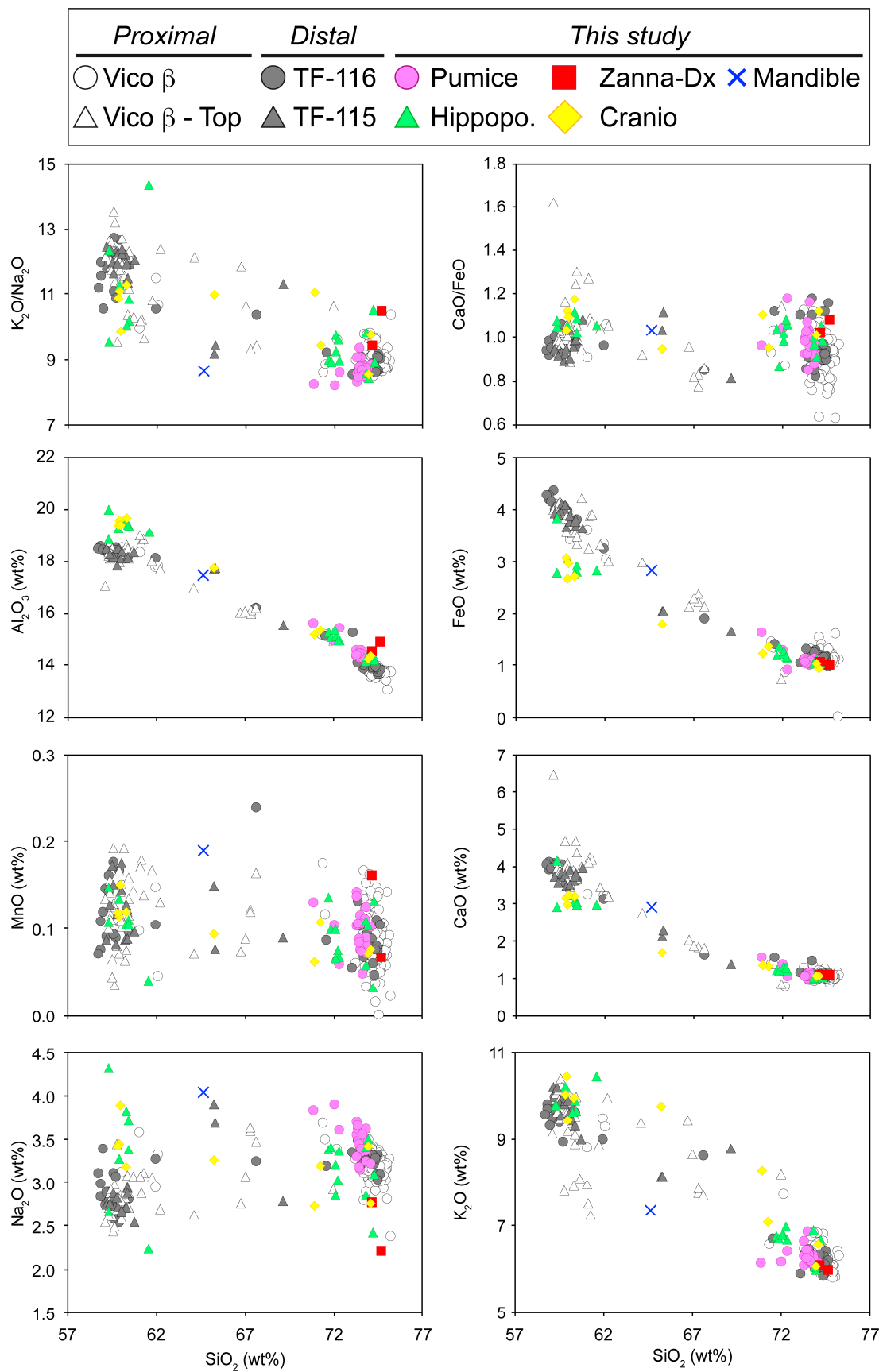
Figure 21. Bi-plot scatter diagrams of the investigated samples in comparison with literature data of Vico diagrams of top proximal deposits and their distal equivalents. Data source: Vico β Data source: [128]; TF-116 and TF-115: [149].
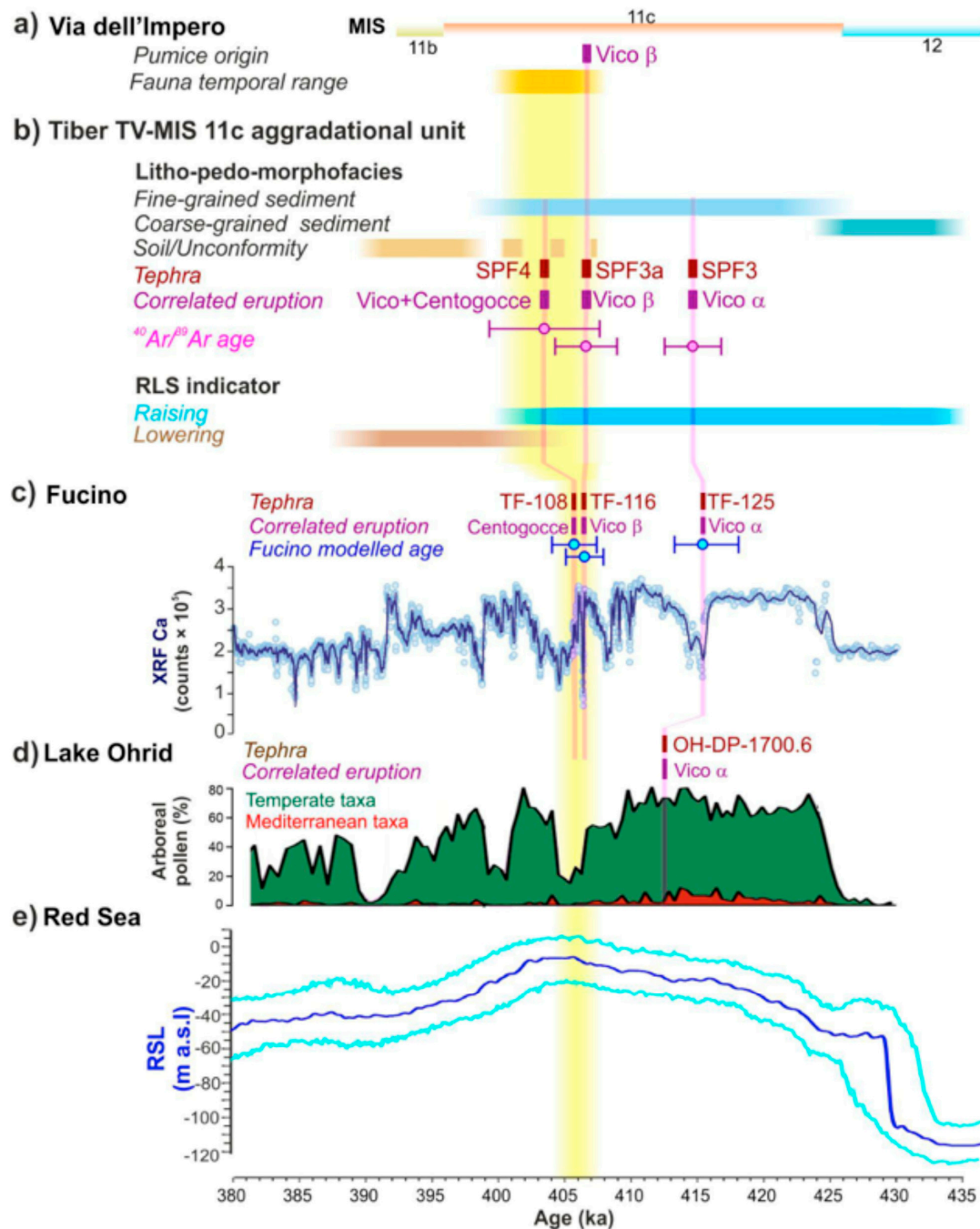
Figure 22. Chronological and paleoenvironmental-paleoclimatic setting of Via dell'Impero faunal remains. (**a**) Origin and age of the pumice samples extracted from the sediment adhering to the surface of Via dell'Impero mammal bones and temporal range of the paleontological findings; (**b**) Stratigraphy, geochronology and sea-level indicators of the MIS 11c aggradational unit of the Tiber River paleo-delta (from [131]); (**c**) MIS 11 temporal series of the calcium content in Fucino paleolake record [151]; (**d**) Lake Ohrid MIS 11 pollen profile [138]; (**e**) Red Sea MIS 11 Relative seal level (RSL) based on the "Red Sea method" [149].

4.4. The Via dell'Impero Mammals in Framework of the Middle Pleistocene (MIS 13-MIS 7) Mammalian Fauna from Latium

The VFI large mammal fauna includes a few remains belonging to five species, *P. antiquus*, *H.* cf. *antiquus*, *C. elaphus*, a fallow deer specimen showing some similarities with the Clacton deer, and *B. primigenius*. The VFI species have little biochronological

significance, except for the long-lasting Villafranchian species *H. antiquus* that has not been certainly reported in the Latium LFAs after MIS 11. During MIS 11, *H. antiquus* populations might have shared the suitable habitat with *H. amphibius* that seems to have already inhabited the Campagna Romana ([86], but see [38], and references therein). The chronological range of other species extends before and after MIS 11 (Figure 23).
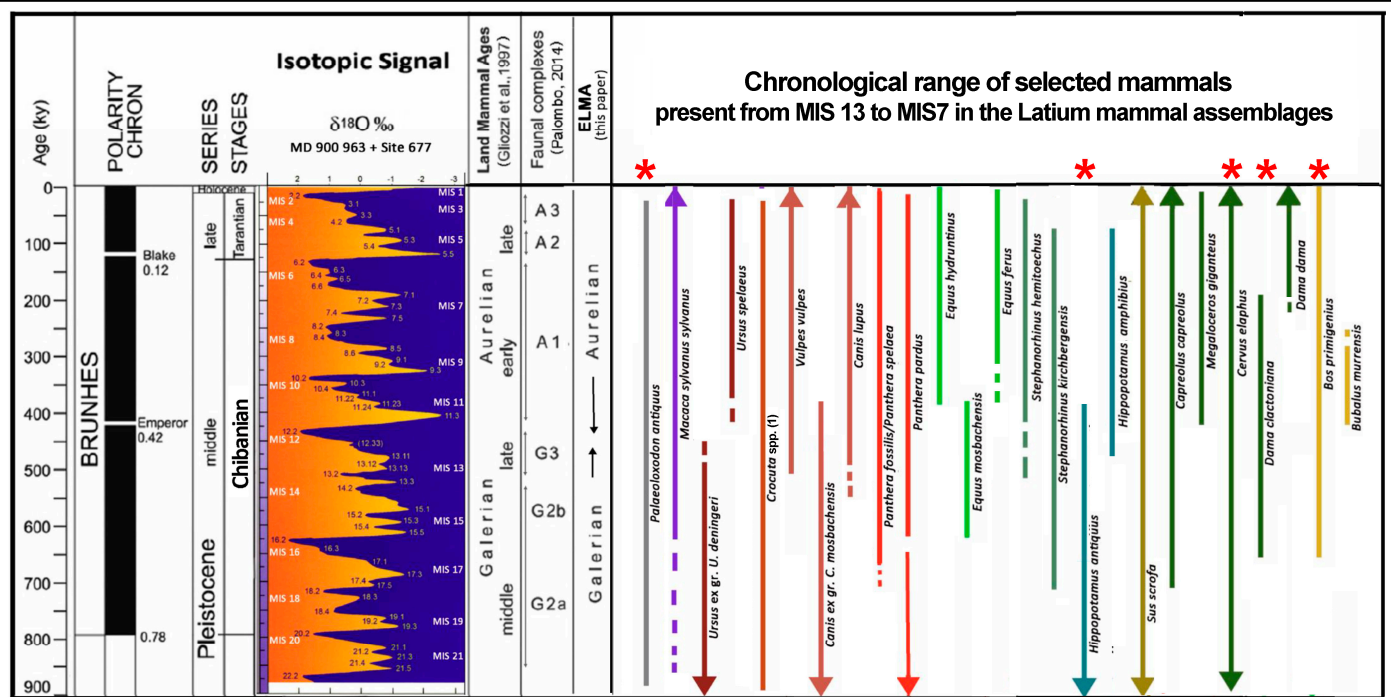
Figure 23. Chronological range of the large mammal species recorded in western and southern Europe during the Middle Pleistocene (Land mammal Ages and Faunal Complex after [92] and [93], respectively). The asterisk indicates those of the species discovered in 1932 at the Vela hill's slope bottom, during the excavation works for the opening of Via dell'Impero.

The VFI mammal remains were retrieved from attritional fluvial deposits, filling a paleovalley incised into older deposits during sea and base level falls. The paleovalley is part of a large network of diversely oriented incised valleys, whose evolution was regulated by sea-level oscillations. These oscillations affected the base level fall and lowstand (valley incision), and the base level rise and highstand (valley filling) in the frame of the slow uplifting of the Basin of Rome (e.g., [24,153]).

Similarly to VFI mammal remains, most of the mammal fossil assemblages of the Latium area were discovered within deposits filling incised valleys. Some remains were progressively accumulated on the river bottom after short- or long-distance transport. The transportation of these remains potentially included elements that have been reworked from older deposits; some assemblages were the result of rapid bone accumulation associated with flooding events; other comprised remains that were accumulated within lacustrine sediments, or in stagnant and muddy waters of swampy environments, and rarely in peri-lacustrine deposits during minor oscillations of the lake level. Occasionally, bones have been transported by lahars and deposited not far from the volcanic complex where the lahars originated. Therefore, the richness, composition, and structure of LFAs mainly depend on the nature of the deposition, the taphonomic context, and the sedimentary processes that shaped the bone accumulation, burial, and preservation. The latter factors greatly influenced the taxonomic configuration of the assemblages. However, the fossil assemblages may not be faithful to the original compositions and structure of the paleocommunities that inhabited the territory at the time of bone accumulation and may vary from an LFA to another even if the structure of paleocommunities remains substan-

tially unaltered. Sometimes, the LFA richness and diversity are particularly low, and the fauna might consist of remains particularly resistant to potentially damaging biostratinomic processes, such as teeth or long bones. Remains of species that had a high density on the territory surrounding the site, such as gregarious large mammals, in particular herbivores, might also be overrepresented in the fossil record with respect to the rare species or those living solitary or forming small herds.

The synergetic action of several factors (e.g., depositional setting, paleoenvironmental conditions, species ecological flexibility and requirements, and taphonomic and/or random factors) accounts for the disparities in richness and diversity of the Latium LFAs (Table 2), which are dominated by the most commonly found species, straight-tusked elephant, red deer, and aurochs. The same species are recorded in the VFI LFA (Figure 24). Among the analyzed LFAs, the richest is Fontana Ranuccio (15 species) (MIS 11c) [113], which includes the "Galerian" species *Ursus deningeri*, followed by the assemblages of the lower (12 species) and upper (14 species) fossiliferous layers of Torre in Pietra deposited during MIS 9 and MIS 7 [26], respectively. On average, the MIS 11 LFAs are less rich than the more recent (MIS 9-MIS 7) and a few, including the VFI one, count less than six species, which is the minimum number of taxa recorded in the selected MIS 9-MIS 7 LFAs.
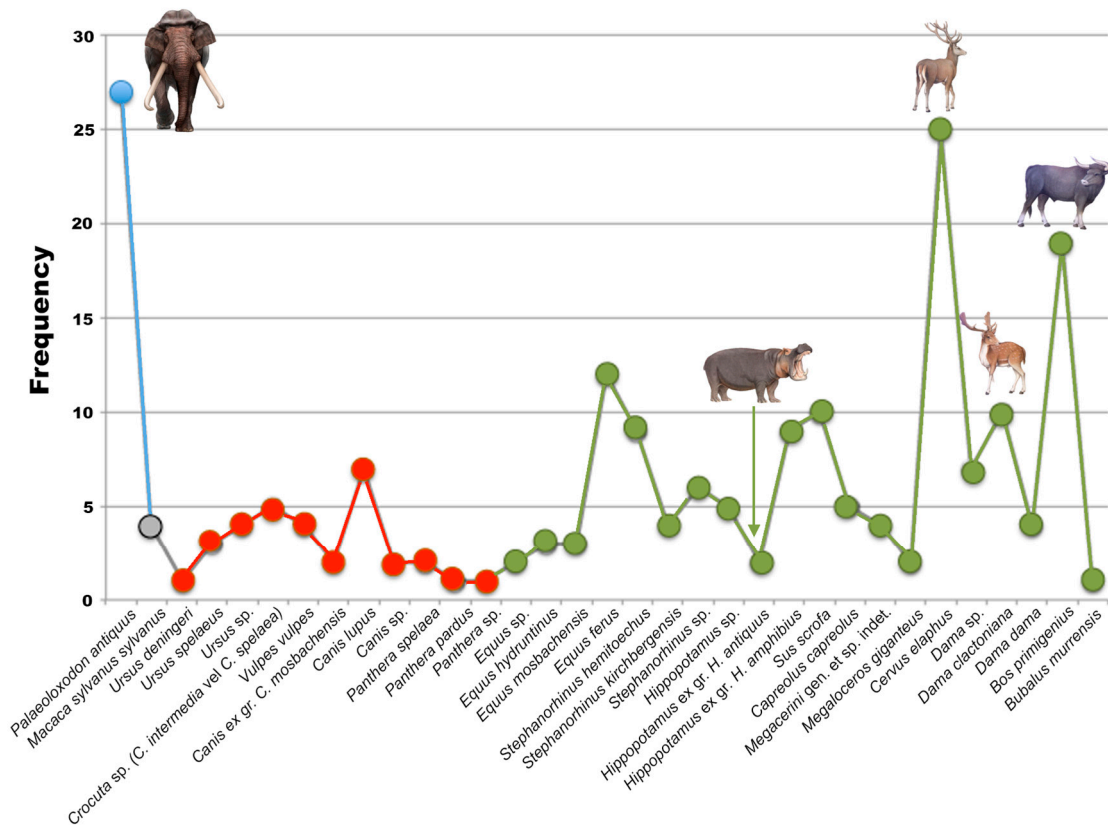
Figure 24. Commonness of the large mammal species recorded in the local faunal assemblages selected for this study (see Table 1). Mammal miniatures indicate the species identified in the VFI fauna assemblage.

The effect caused by the depositional context and by related taphonomic biases may be accountable for the commonness of the taxa recorded in almost all local assemblages, the low number of rich and diversified faunal assemblages, and some faunal monotony. Indeed, the cluster analysis failed to provide any clues for chronologically discriminating the LFAs herein examined. In the dendrogram resulting from the analysis (Figure 25), all LFAs gather together in a single large cluster (A), except for Casal Selce 2 [103] and Via Ostiense [112], each forming a separate branch. This result is expected since only a single species is recorded at each site, *Canis lupus* and *C. mosbachensis*, respectively, whilst no one

among the most common species has been recorded so far. Among these species, only *P. antiquus* is recorded at the Foresta-Devil's trails ichnosite (also known as Ciampate del Diavolo) [154] which falls into the cluster A. However, the Foresta-Devil's trails ichnosite diverges from the group A1 in a separate ramus. A1 includes a large group, A1.1, from which diverges the ramus of the MIS 13 LFA, which is retrieved from the lower levels of the Casal Selce site. A1.1 includes two sister clusters, the very small cluster A1.1.2 gathering only two MIS 13 LFAs, and the large cluster A.1.1.1, gathering all other LFAs. However, in the large group A1.1.1.1, most of the LFAs ranging in age from MIS 11 to MIS 10 and from MIS 9 to MIS 7 gather separately in the sister clusters A1.1.1.1.1 and A1.1.1.1.2, respectively (Figure 25).
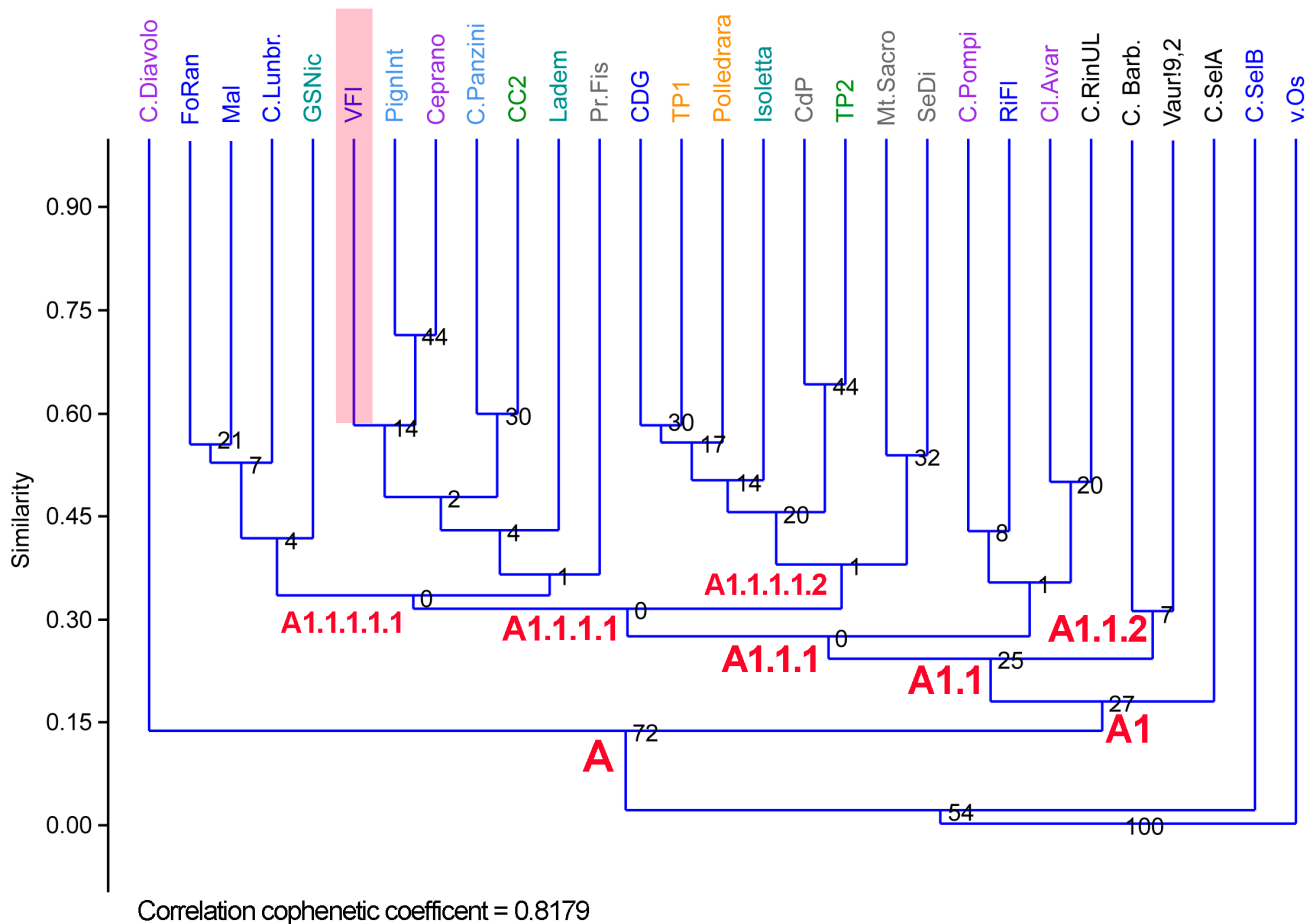
Figure 25. Q-mode dendrogram showing the hierarchical ordering obtained for the late Middle Pleistocene (MIS 13-MIS 7) local faunal assemblages from Latium and surrounding areas, selected among the best-known LFAs, having some chronological constraints. Clusters are joined based on the average distance between all members in the groups (unweighted pair-group average, UPGMA). Black = Mis 13; Blue = Mis 11; Azure = MIS 11 or younger; Dark green = late MIS 11–early MIS 10; Violet = MIS 10; Yellow = MIS 9; Grey = MIS 8.5; Light green = MIS 7. C.Diavolo = Ciampate del Diavolo; FoRan = Fontana Ranuccio; Mal = Malagrotta; C Lumbr. = Casal Lumbroso; GC-Nic = Guado San Nicola; VFI = Via dell'Impero/Via dei Fori Imperiali; Pignint = Pignataro Interamna; Ceprano = Ceprano CG 9–10; CC2 = Campo di Conte upper levels; Ladem = Lademagne levels 1 and 2; Pr.Fis = Prati Fiscali; CDG = Castel di Guido; TP1 = Torre in Pietra lower levels; Polledrara = Polledrara di Cecanibbio; Isoletta = Isoletta (ESR1-GA6Z-ESR4); CdP = Casal de' Pazzi; TP2 = Torre in Pietra upper levels; Mt.Sacro = Monte Sacro; SeDi = Sedia del Diavolo; C.Pompi = Cava Pompi; RiFi = Rio Freddo; ClAvar = Colle Avarone; C.RinUl = Cava Rinaldi upper levels; CBarb = Collina Barbattini; Vaur9.2 = Via Aurelia Km 9.2; C.SelA = Casal Selce lower levels = C.SelB = Casal Selce upper Level; V.Os = Via Ostiense.

Accordingly, the LFA clustering mainly depends on the presence of high frequent species whose remains are generally easily identifiable (*P. antiquus*, *Cervus elaphus*, and *Bos primigenius*) more than on the fauna richness or some chronological differences among sites. Indeed, the dendrogram does not show any reliable chronological order. Nonetheless, the hierarchical assessment of the LFAs herein selected for the analysis reveals the tendency to cluster separately of the MIS 13 LFA, underlining some substantial uniformity of LFAs ranging from MIS 11 to MIS 7 (Aurelian ELMA, *sensu* [93]).

Moreover, the lack of studies on the autecology of taxa recorded at each site and of stable and unstable isotope data hampers the evaluation of their putatively significant differences among sites in different paleoenvironmental conditions (temperature, humidity, and vegetation cover). For instance, more in-depth studies of the faunal assemblages were done for La Polledrara di Cecanibbio and Casal de' Pazzi LFAs [72,73]. Moreover, the comparison among the habit, trophic, and body mass structure of Latium LFA ranging in age from MIS 13 to MIS 7 LFAs has evidenced a high variability among the relative abundance of ecological groups present in each local large mammal assemblage ([155], Figures 5 and 6). However, the comparison failed to detect any informative differences between LFAs, giving only general indications about the presence on the territory of environments with a mixed vegetation cover (grasslands, wooded grasslands, and woodlands). Unfortunately, data on the Latium vegetation cover in the MIS 11 sites that yielded mammal remains do not provide further support for the LFAs paleoenvironmental reconstruction. The data available for MIS 11 sites yielding large mammal assemblages are limited to the macrovegetation of the Riano Flaminio (Rome) [69] and the pollen record of the lowest levels of the Isoletta's stratigraphic sequence (lacustrine phase, MIS 11) (Frosinone) [156]. Indeed, the data on the pollen sequences from Fontana Ranuccio [157] and Ceprano [158] refer to levels underlying the fossiliferous ones. The Riano Flaminio macroflora indicates the presence of a rather dense and humid forest, while the Isoletta pollen record suggests a prevalent presence of conifers and deciduous wooded areas, as well as some open landscapes.

All things considered, the substantial uniformity of the Latium LFAs, ranging in age from MIS 11 to MIS 7, underlines the difficulties in detecting and defining low-rank biochronological units (i.e., Faunal Units) for large mammalian assemblages found in fossiliferous layers spanning a short geological time, such as the about 230 ka encompassed by the MIS 11-MIS 7 late Middle Pleistocene (Aurelian ELMA *sensu* [93]). However, these LFAs are of some biochronologic, ecologic, and ethologic relevance because they document the contemporaneous presence during MIS 11 and on the same territory of *Canis lupus* and *Canis mosbachensis* populations [108,112] and, maybe, that of the Villafranchian *H. antiquus*, also recorded in the VFI LFA, and *H. amphibius* ([86], but see, [38], and references therein). Furthermore, on the one hand, *E. mosbachensis* could be present till the beginning of MIS 10 (Table 2). On the other hand, LFA lists of several Latium sites, ranging in age from MIS 11 to MIS 7, report the presence of *Equus ferus*. If confirmed, this would imply the contemporaneous presences of two caballine horses at list during MIS 11. However, most of the alleged *E. ferus* remains lack a formal description, and their identification is doubtful ([159], and references therein). Therefore, the precise time of the actual appearance in the Latium area of the latter species is unknown, though attested during MIS 9 by the presence of a rather rich sample of *E. ferus* remains from the lower level of the Torre in Pietra, for which Caloi [160,161] proposed the alleged subspecies, *E. ferus malatestae*.

Overall, the stratigraphic data derived from incised valley fills interspersed with pyroclastic deposits, along with the correlation of unconformity-bounded stratigraphic successions, radiometric dating, and tephrochronology provide significant constraints for establishing a robust chronological framework for these LFAs. This is particularly relevant for those LFAs that include the remains of several frequently documented species, such as the VFI LFA.

5. Conclusions

This research analyzes, for the first time, the large mammal assemblage discovered in 1932 during the construction work of Via dell'Impero (VFI). Some years after their rescue, fossils and VFI material were transferred partly to the Museum of Roman Civilization, partly to the management of the Musei Capitolini, and partly elsewhere in Rome. For a long time, the material was apparently forgotten and believed lost by many scholars. Recently, the Capitoline Superintendence re-discovered part of the fossil material collected at VFI, allowing their first and detailed study [42]. The study of the fossil assemblage here carried out updates the identification already proposed by De Angelis d'Ossat [40], confirming the presence in the LFA of *P. antiquus*, *C. elaphus*, and *B. primigenius*, but attributing the remains of hippopotamus to *H.* cf. *antiquus* and a fragment of burr to *Dama* sp.

Moreover, the research analyzes for the first time the composition in major elements of a pumice retrieved from the VFI fossiliferous layers and of the ash extracted from some samples of sediments still adhering to the surface of the mammalian bones. The integration of geochemical data from volcanic products with faunal remains is essential for correctly arranging the stratigraphic sequences to support the current chronological framework of the Rome Basin LFAs. These data allow researchers to discriminate between products deriving from well-dated volcanic events, thereby providing compelling geochronological data that serves as a *terminus post quem* for the sediments and the accumulation of mammal remains.

All the herein analyzed glass of the pumices extracted from the VFI samples are K-rich rhyolites, which is a quite rare composition within the framework of the peri-Tyrrhenian ultrapotassic volcanism and a peculiar feature of the products of early explosive activity of the Vico volcano. Specifically, among the two geochemically similar Vico α (414.8 ± 2.2 ka) and Vico β (406.5 ± 2.4 ka) Plinian units, all VFI samples show a stronger affinity with the younger Vico β unit. This, alongside the tephra correlation with the Fucino record, allowed us to precisely constrain the VFI fossiliferous level. The latter was most likely deposited within the short temporal range spanning between <406.5 ± 1.3 ka and >405.7 + 1.5/−1.6 ka, in agreement with the attribution to the Torrino Formation of the VFI levels already proposed by Mancini and colleagues [162].

The results of this research underline once again that LFAs, including taxa with little chronological and moderate ecological relevance, can be correctly integrated within the evolutionary and paleoenvironmental dynamics of a territory only when supported by compelling chronological constraints. This is particularly useful in the case of large mammal faunas of the Middle Pleistocene post Mid-Brunhes event (MIS 11-MIS 7), a period lacking significant faunal renewals. During that time, the Latium LFAs were often dominated by common species (elephant, red deer, aurochs) with broad biochronological ranges and moderate ecological flexibility, requiring a multidisciplinary approach to extrapolate paleoecological information.

Acronyms and Abbreviation

AB	anterior breath
BD	distal breadth
Bfi	inner breadth of the rostral fan
Bfo	outer breadth of the rostral fan
DD	distal depth
VFI	Via dell'Impero, now Via dei Fori Imperiali
AD-MCR	Antiquarium Depositorium at Museo della Civiltà Romana
McT	Mercati di Traiano
F	average lamellar frequency
Foccl	occlusal lamellar frequency
L	maximum length
LFl	lateral lamellar frequency
LFm	medial lamellar frequency
LS	length of the mandibular symphysis
PB	posterior breadth

References

1. Webb, S.D.; Opdyke, N.D. Global climatic influence on Cenozoic land mammal faunas. In *Effects of Past Global Change on Life*; National Research Council, Division on Earth, Life Studies, Commission on Geosciences, Panel on Effects of Past Global Change on Life, Eds.; The National Academies Press: Washington, DC, USA, 1995; pp. 184–208.
2. Carotenuto, F.; Di Febbraro, M.; Melchionna, M.; Castiglione, S.; Saggese, F.; Serio, C.; Mondanaro, A.; Passaro, F.; Loy, A.; Raia, P. The influence of climate on species distribution over time and space during the late Quaternary. *Quat. Sci. Rev.* **2016**, *149*, 188–199. [CrossRef]
3. Van Dam, J.A.; Abdul Aziz, H.; Angeles Alvarez Sierra, M.; Hilgen, F.J.; van den Hoek Ostende, L.W.; Lourens, L.J.; Mein, P.; van der Meule, A.J.; Pelaez-Campomanes, P. Long-period astronomical forcing of mammal turnover. *Nature* **2006**, *443*, 687–691. [CrossRef] [PubMed]
4. Barnosky, A.D.; Kraatz, B.P. The role of climatic change in the evolution of mammals. *Bioscience* **2007**, *57*, 523–532. [CrossRef]
5. Levinsky, I.; Skov, F.; Svenning, J.C.; Rahbek, C. Potential impacts of climate change on the distributions and diversity patterns of European mammals. *Biodivers. Conserv.* **2007**, *16*, 3803–3816. [CrossRef]
6. Hofreiter, M.; Stewart, J. Ecological change, range fluctuations and population dynamics during the Pleistocene. *Current Biol.* **2009**, *19*, R584–R594. [CrossRef]
7. Post, E.; Brodie, J.; Hebblewhite, M.; Anders, A.D.; Maier, J.A.M.; Wilmers, C.C. Global population dynamics and hot spots of response to climate change. *BioScience* **2009**, *59*, 489–497. [CrossRef]
8. Holm, S.R.; Svenning, J.C. 180,000 years of climate change in Europe: Avifaunal responses and vegetation implications. *PLoS ONE* **2014**, *9*, e94021. [CrossRef]
9. Palombo, M.R. Deconstructing mammal dispersals and faunal dynamics in SW Europe during the Quaternary. *Quat. Sci. Rev.* **2014**, *96*, 50–71. [CrossRef]
10. Palombo, M.R. Discrete dispersal bioevents of large mammals in Southern Europe in the post-Olduvai Early Pleistocene: A critical overview. *Quat. Int.* **2017**, *431*, 3–19. [CrossRef]
11. Jackson, S.T.; Blois, J.L. Community ecology in a changing environment: Perspectives from the Quaternary. *Proc. Natl. Acad. Sci. USA* **2015**, *112*, 4915–4921. [CrossRef]
12. Schreve, D. All is flux: The predictive power of fluctuating Quaternary mammalian faunal-climate scenarios. *Philos. Trans. R. Soc. B* **2019**, *374*, 20190213. [CrossRef] [PubMed]
13. Lindsay, E.H. Chapter 10: Chronostratigraphy, Biochronology, Datum Events, Land Mammal Ages, Stage of Evolution, and Appearance Event Ordination. In *Bulletin of the American Museum of Natural History*; BioOne: Washington, DC, USA, 2003; pp. 212–230.
14. Palombo, M.R. Biochronology of terrestrial mammals and Quaternary subdivisions: A case study of large mammals from the Italian peninsula. *Alp. Mediterr. Quat.* **2009**, *22*, 291–306.

15. Palombo, M.R. Large mammals faunal dynamics in southwestern Europe during the late Early Pleistocene: Implications for the biochronological assessment and correlation of mammalian faunas. *Alp. Mediterr. Quat.* **2016**, *29*, 143–168.

16. Nomade, S.; Pastre, J.F.; Guillou, H.; Faure, M.; Guérin, C.; Delson, E.; Debard, E.; Voinchet, P.; Messager, E. 40Ar/39Ar constraints on some French landmark Late Pliocene to Early Pleistocene large mammalian paleofaunas: Paleoenvironmental and paleoecological implications. *Quat. Geochr.* **2014**, *21*, 2–15. [CrossRef]

17. Branca, S.; Cinquegrani, A.; Cioni, R.; Conte, A.M.; Conticelli, S.; De Astis, G.; de Vita, S.; De Rosa, R.; Di Vito, M.A.; Donato, P.; et al. The Italian Quaternary volcanism. *Alp. Mediterr. Quat.* **2023**, *36*, 221–284.

18. Milli, S. Depositional setting and high-frequency sequence stratigraphy of the Middle-Upper Pleistocene to Holocene deposits of the Roman Basin. *Geol. Romana* **1997**, *33*, 99–136.

19. Milli, S. The sequence stratigraphy of the Quaternary successions: Implications about the origin and filling of incised valleys and the mammal fossil record. In *Workshop Thirty Years of Sequence Stratigraphy: Applications, Limits and Prospects*; Sabato, L., Spalluto, L., Tropeano, M., Eds.; Geosed: Bari, Italy, 2006; pp. 27–28.

20. Milli, S.; Moscatelli, M.; Palombo, M.R.; Parlagreco, L.; Paciucci, M. Incised-valleys, their filling and mammal fossil record: A case study from Middle-Upper Pleistocene deposits of the Roman Basin (Latium, Italy). *GeoActa Spec. Publ.* **2008**, *1*, 67–88.

21. Marra, F.; Florindo, F. The subsurface geology of Rome: Sedimentary processes, sea-level changes and astronomical forcing. *Earth-Sci. Rev.* **2014**, *136*, 1–20. [CrossRef]

22. Marra, F.; Florindo, F.; Anzidei, M.; Sepe, V. Paleo-surfaces of glacio-eustatically forced aggradational successions in the coastal area of Rome: Assessing interplay between tectonics and sea-level during the last ten interglacials. *Quat. Sci. Rev.* **2016**, *148*, 85–100. [CrossRef]

23. Luberti, G.M.; Marra, F.; Florindo, F. A review of the stratigraphy of Rome (Italy) according to geochronologically and paleomagnetically constrained aggradational successions, glacio-eustatic forcing and volcano-tectonic processes. *Quat. Int.* **2017**, *438*, 40–67. [CrossRef]

24. Milli, S.; Palombo, M.R. The high-resolution sequence stratigraphy and the mammal fossil record: A test in the Middle–Upper Pleistocene deposits of the Roman Basin (Latium, Italy). *Quat. Int.* **2005**, *126*, 251–270. [CrossRef]

25. Palombo, M.R.; Milli, S. Mammal fossil record, depositional setting, and sequence stratigraphy in the Middle-Upper Pleistocene of Roman Basin. *Il Quaternario. Ital. J. Quat. Sci.* **2010**, *23*, 257–262.

26. Villa, P.; Soriano, S.; Grün, R.; Marra, F.; Nomade, S.; Pereira, A.; Boschian, G.; Pollarolo, L.; Fang, F.; Bahain, J.J. The Acheulian and early Middle Paleolithic in Latium (Italy): Stability and innovation. *PLoS ONE* **2016**, *11*, e0160516. [CrossRef] [PubMed]

27. Pereira, A.; Nomade, S.; Falguères, C.; Bahain, J.-J.; Tombret, O.; Garcia, T.; Voinchet, P.; Bulgarelli, G.M.; Anzide, A.P. 40Ar/39Ar and ESR/U-series data for the La Polledrara di Cecanibbio archaeological site (Lazio, Italy). *J. Archaeol. Sci. Rep.* **2017**, *15*, 20–29. [CrossRef]

28. Romano, M.; Avanzini, M. The skeletons of Cyclops and Lestrigons: Misinterpretation of Quaternary vertebra-tes as remains of the mythological giants. *Hist. Biol.* **2019**, *31*, 117–139. [CrossRef]

29. Kotsakis, T.; Barisone, G. Cenni sui vertebrati fossili di Roma. *Mem. Descr. Carta Geol. It.* **2008**, *80*, 115–143.

30. Palombo, M.R. Elefanti a Roma. In *Quando a Roma Vivevano Gli Elefanti*; Gioia, P., Ed.; Rubettino: Rome, Italy, 2020; pp. 112–119.

31. Romano, M.; Mecozzi, B.; Sardella, R. The Quaternary paleontological research in the Campagna Romana (central Italy) at the 19th-20th century transition. Historical overview. *Alp. Mediterr. Quat.* **2021**, *34*, 109–130.

32. Sergi, S. La scoperta di un cranio del tipo di Neanderthal presso Roma. *Riv. Antropol.* **1929**, *28*, 457–462.

33. Breuil, H.; Blanc, A.C. Ritrovamento "in situ" di un nuovo cranio di "*Homo neanderthalensis*" nel giacimento di Saccopastore (Roma). *Rend. R. Accad. Naz. Lincei Cl. Sci. FMN* **1935**, *6*, 166–169.

34. Arnoldus-Huyzendveld, A.; Zarlenga, F.; Gioia, P.; Palombo, M.R. Distribution in space and time and analysis of preservation factors of Pleistocene deposits in the Roman area. In *The World of Elephants*; Cavarretta, G., Gioia, P., Mussi, M., Palombo, M.R., Eds.; CNR Editions: Rome, Italy, 2001; pp. 10–17.

35. Caloi, L.; Manzi, G.; Palombo, M.R. Saccopastore, Roma: Problemi di cronologia e di interpretazione del sito. In Proceedings of the XIII Convegno Della Società Paleontologica Italiana, Parma, Italy, 10–13 September 1996; p. 80.

36. Bruner, E.; Manzi, G. Saccopastore 1: The earliest Neanderthal? A new look at an old cranium. In *Neanderthals Revisited: New Approaches and Perspectives*; Springer: Berlin/Heidelberg, Germany, 2006; pp. 23–36.

37. Marra, F.; Ceruleo, P.; Jicha, B.; Pandolfi, L.; Petronio, C.; Salari, L. A new age within MIS 7 for the Homo neanderthalensis of Saccopastore in the glacio-eustatically forced sedimentary successions of the Aniene River Valley, Rome. *Quat. Sci. Rev.* **2015**, *129*, 260–274. [CrossRef]

38. Martino, R.; Marra, F.; Ríos, M.I.; Pandolfi, L. The Middle Pleistocene *Hippopotamus* from Malagrotta (Latium, Italy): New Data and Future Perspectives. *Quaternary* **2023**, *7*, 13. [CrossRef]

39. De Angelis D'Ossat, G. Prime notizie sui fossili rinvenuti fra la Basilica Costantiniana ed il Colosseo. *Atti Pontif. Accad. Sci. N. Lincei* **1932**, *85*, 373–376.

40. De Angelis D'Ossat, G. Il sottosuolo dei Fori Romani e l'*Elephas antiquus* della Via dell'Impero. *Bull. Comm. Arch. Com. Roma* **1935**, *63*, 1–34.

41. Parisi Presicce, C.; Bernacchio, N.; Damiani, I.; Fogagnolo, S.; Munzi, M. *1932. L'elefante e il colle perduto (catalogo della mostra)*; Roma Culture e Sovrintendenza Capitolina ai Beni Culturali, Campisano Editore: Rome, Italy, 2022; 64p.

42. Palombo, M.R.; Pandolfi, L. La riscoperta del celebre cranio di elefante antico di Via dell'Impero. In *Materiali e Documenti Dalla Collina Velia. Scoperte 1932*; Parisi Presicce, C., Damiani, I., Del Moro, P., Munzi, M., Eds.; Supplemento in Bullettino della Commissione Archeologica Comunale: Rome, Italy, *in press*.

43. Lister, A.M.; Van Essen, H. Mammuthus rumanus (Stefanescu), the earliest mammoth in Europe. In *Advances in Vertebrate Paleontology "Hen to Panta"*; Petculescu, A., Stiuca, E., Eds.; Romanian Academy, 'Emil Racovita' Institute of Speleology: Bucharest, Romania, 2003; pp. 46–52.

44. Aguirre, E.E. Revisión sistemática de los Elephantidae por su morfología y morfometría dentaria. *Estud. Geol.* **1969**, *25*, 123–177 & 317–367.

45. Maglio, V.J. Origin and evolution of the Elephantidae. *Trans. Am. Philos. Soc.* **1973**, *63*, 1–149. [CrossRef]

46. Lister, A.M. Evolution and taxonomy of Eurasian mammoths. In *The Proboscidea: Evolution and Palaeoecology of Elephants and Their Relatives*; Shoshani, J., Tassy, P., Eds.; Oxford University Press: Oxford, UK, 1996; pp. 203–213.

47. Mazza, P. New Evidence on the Pleistocene Hippopotami of Western Europe. *Geol. Romana* **1995**, *31*, 61–241.

48. Heintz, E. Les cervidés villafranchiens de France et d'Espagne. *Mém. Mus. Nation. Hist. Natur. Série C Sci. Terre* **1970**, *22*, 1–303.

49. Driesch, A.v.d. *A Guide to the Measurements to Animal Bones from Archaeological Sites*; Peabody Museum Bull Harvard University: Cambridge, MA, USA, 1976; pp. 1–137.

50. Hair, F., Jr.; Anderson, R.E.; Tatham, R.L.; Black, W.C. *Multivariate Data Analysis*; Prentice Hall: Upper Saddle River, NJ, USA, 1998.

51. Hammer, Ø.; Harper, D.; Ryan, P.D. Past: Paleontological Statistics Software Package for Education and Data Analysis. *Palaeontol. Electron.* **2001**, *4*, 9.

52. Lê, S.; Josse, J.; Husson, F. FactoMineR: An R package for multivariate analysis. *J. Stat. Softw.* **2008**, *25*, 1–18. [CrossRef]

53. Vu, V.Q. Ggbiplot: A Ggplot2 Based Biplot, R Package Version 0.55. 2011. Available online: http://github.com/vqv/ggbiplot (accessed on 1 November 2023).

54. Husson, F.; Josse, J.; Le, S.; Mazet, J.; Husson, M.F. Package 'factoMineR'. An R Package. 2017. Available online: https://CRAN.R-project.org/package=FactoMineR (accessed on 1 November 2023).

55. Tang, Y.; Horikoshi, M.; Li, W. Ggfortify: Unified interface to visualize statistical results of popular R packages. *R J.* **2016**, *8*, 474. [CrossRef]

56. Kassambara, A.; Mundt, F. Package 'Factoextra.' Extract and Visualize the Results of Multivariate Data Analyses, R Package Version 1.0.7. 2017. Available online: https://CRAN.R-project.org/package=factoextra (accessed on 1 November 2023).

57. R Core Team, R. *A Language and Environment for Statistical Computing*; R Foundation for Statistical Computing: Vienna, Austria, 2019.

58. Jochum, K.P.; Stoll, B.; Herwig, K.; Willbold, M.; Hofmann, A.W.; Amini, M.; Aarbug, S.; Abouchami, W.; Hellebrand, E.; Mocek, B.; et al. MPI-DING reference glasses for in situ microanalysis: New reference values for element concentrations and isotope ratios. *Geochem. Geophys.* **2006**, *7*, 2. [CrossRef]

59. Le Maitre, R.W.; Streckeisen, A.; Zanettin, B.; Le Bas, M.J.; Bonin, B.; Bateman, P.; Bellieni, G.; Dudek, A.; Efremova, S.; Keller, J.; et al. *Igneous Rocks: A Classification and Glossary of Terms. Reccomendation of the International Union of Geological Sciences Subcommission on the Systematics of Igneous Rocks*, 2nd ed.; Cambridge University Press: Cambridge, MA, USA, 2002; 236p.

60. Sher, A.V.; Garutt, V.E. New data on the morphology of elephant molars. *Trans. USSR Acad. Sci. Earth Sci. Sect.* **1987**, *285*, 195–199.

61. Lister, A.M.; Sher, A.V. Evolution and dispersal of mammoths across the Northern Hemisphere. *Science* **2015**, *350*, 805–809. [CrossRef] [PubMed]

62. Albayrak, E.; Lister, A.M. Dental remains of fossil elephants from Turkey. *Quat. Int.* **2012**, *276*, 198–211. [CrossRef]

63. Palombo, M.R.; Ferretti, M.P. Elephant fossil record from Italy: Knowledge, problems, and perspectives. *Quat. Int.* **2005**, *126*, 107–136. [CrossRef]

64. Larramendi, A.; Zhang, H.; Palombo, M.R.; Ferretti, M.P. The evolution of *Palaeoloxodon* skull structure: Disentangling phylogenetic, sexually dimorphic, ontogenetic, and allometric morphological signals. *Quat. Sci. Rev.* **2020**, *229*, 106090. [CrossRef]

65. Bon, M.; Piccoli, G.; Sala, B. La fauna pleistocenica della breccia di Slivia (Carso Triestino) nella collezione del Museo civico di Storia naturale di Trieste. *Atti Mus. Civ. Stor. Nat. Trieste* **1992**, *44*, 33–51.

66. Sala, B.; Masini, F. Late Pliocene and Pleistocene small mammal chronology in the Italian peninsula. *Quat. Int.* **2007**, *160*, 4–16. [CrossRef]

67. Palombo, M.R.; Albayrak, E.; Marano, F. The straight-tusked Elephants from Neumark Nord, a glance to a lost world. In *Elefantenreich-Eine Fossilwelt in Europa*; Meller, H., Ed.; Katalog zur Sonderausstellung im Landesmuseum für Vorgeschichte Halle: Halle, Germany, 2010; pp. 219–247.

68. Palombo, M.R. To what extent could functional diversity be a useful tool in inferring ecosystem responses to past climate changes? *Quat. Int.* **2016**, *413*, 15–31. [CrossRef]

69. Follieri, M. La foresta colchica fossile di Riano Romano. I. Studio dei fossili vegetali macroscopici. *Annali Bot.* **1958**, *26*, 129–142.

70. Benvenuti, M.; Bahain, J.J.; Capalbo, C.; Capretti, C.; Ciani, F.; D'Amico, C.; Esu, D.; Giachi, G.; Giuliani, C.; Gliozzi, E.; et al. Paleoenvironmental context of the early Neanderthals of Poggetti Vecchi for the late middle Pleistocene of Central Italy. *Quat. Res.* **2017**, *88*, 327–344. [CrossRef]

71. Magri, D. Il bosco perduto. In *Il Museo di Casal de'Pazzi Racconta Quando a Roma Vivevano Gli Elefanti*; Gioia, P., Ed.; Roma Capitale, Sovrintendenza Capitolina ai Beni Culturali, Rubbettino Editore: Rome, Italy, 2020; pp. 165–169.

72. Palombo, M.R.; Filippi, M.L.; Iacumin, P.; Longinelli, A.; Barbieri, M.; Maras, A. Coupling tooth microwear and stable isotope analyses for palaeodiet reconstruction: The case study of Late Middle Pleistocene *Elephas (Palaeoloxodon) antiquus* teeth from Central Italy (Rome area). *Quat. Int.* **2005**, *126*, 153–170. [CrossRef]

73. Briatico, G.; Gioia, P.; Bocherens, H. Diet and habitat of the late Middle Pleistocene mammals from the Casal de'Pazzi site (Rome, Italy) using stable carbon and oxygen isotope ratios. *Quat. Int.* **2023**, *676*, 53–62. [CrossRef]

74. Roditi, E.; Bocherens, H.; Konidaris, G.E.; Athanassiou, A.; Tourloukis, V.; Karkanas, P.; Panagopoulou, E.; Harvati, K. Life-history of *Palaeoloxodon antiquus* reveals Middle Pleistocene glacial refugium in the Megalopolis basin, Greece. *Sci. Rep.* **2024**, *14*, 1390. [CrossRef]

75. Tsoukala, E.; Mol, D.; Pappa, S.; Vlachos, E.; van Logchem, W.; Vaxevanopoulos, M.; Reumer, J. Elephas antiquus in Greece: New finds and a reappraisal of older material (Mammalia, Proboscidea, Elephantidae). *Quat. Int.* **2011**, *245*, 339–349. [CrossRef]

76. Brugal, J.-P.; Raposo, L. Foz do Enxarrique (Rodao, Portugal): Preliminary results of the analysis of a bone assemblage from a Middle Palaeolithic open site. *Monogr. Römisch-Ger. Zentralmuseums* **1999**, *42*, 367–379.

77. Moussuous, A.; Valensi, P.; Simon, P. Identification de l'ivoire de Proboscidiens des grottes des Balzi Rossi (Ligurie, Italie) à partir de la méthode des lignes de Schreger. *Bull. Mus. Anthropol. Préhist. Monaco* **2014**, *54*, 83–90.

78. Braun, I.M.; Palombo, M.R. *Mammuthus primigenius* in the cave and portable art: An overview with a short account on the elephant fossil record in Southern Europe during the last glacial. *Quat. Int.* **2012**, *276*, 61–76. [CrossRef]

79. Palombo, M.R.; Antonioli, F.; Di Patti, C.; Lo Presti, V.; Scarborough, M.E. Was the dwarfed Palaeoloxodon from Favignana Island the last endemic Pleistocene elephant from the western Mediterranean islands? *Hist. Biol.* **2020**, *33*, 2116–2134. [CrossRef]

80. Theodorou, G.; Symeonidis, N.; Stathopoulou, E. *Elephas tiliensis* n. sp. from Tilos island (Dodecanese, Greece). *Hell. J. Geosc.* **2007**, *42*, 19–32.

81. Pettitt, P.B.; Davies, W.; Gamble, C.S.; Richards, M.B. Palaeolithic radiocarbon chronology: Quantifying our confidence beyond two half-lives. *J. Archaeol. Sci.* **2003**, *30*, 1685–1693. [CrossRef]

82. Caloi, L.; MR, P.; Petronio, C. Resti Cranici Di *Hippopotamus antiquus* (=*H. major*) e *Hippopotamus amphibius* Conservati Nel Museo Di Paleontologia Dell'Università Di Roma. *Geol. Romana* **1980**, *19*, 91–119.

83. Fidalgo, D.; Madurell-Malapeira, J.; Martino, R.; Pandolfi, L.; Rosas, A. An Updated Review of The Quaternary *Hippopotamus* Fossil Records from the Iberian Peninsula. *Quaternary* **2024**, *7*, 4. [CrossRef]

84. Martino, R.; Marra, F.; Beccari, V.; Ríos, M.I.; Pandolfi, L. Middle Pleistocene *Hippopotamus amphibius* (Mammalia, Hippopotamidae) from Southern Europe: Implications for Morphology, Morphometry and Biogeography. *Quat. Sci. Rev.* **2024**, *331*, 108613. [CrossRef]

85. Martino, R.; Zanolli, C.; Fidalgo, D.; Pandolfi, L. Talking Heads: Disentangling the Shape Changes of the Large Extant *Hippopotamus* during Its Ontogenetic Development. *Integr. Zool.* 2024, *in press*. [CrossRef]

86. Mecozzi, B.; Iannucci, A.; Mancini, M.; Tentori, D.; Cavasinni, C.; Conti, J.; Messina, M.Y.; Sarra, A.; Sardella, R. Reinforcing the Idea of an Early Dispersal of *Hippopotamus amphibius* in Europe: Restoration and Multidisciplinary Study of the Skull from the Middle Pleistocene of Cava Montanari (Rome, Central Italy). *PLoS ONE* **2023**, *18*, e0293405. [CrossRef]

87. Di Stefano, G.; Petronio, C. Importance of the morphological plasticity of *Cervus elaphus* in the biochronology of the Middle and Late Pleistocene of the Italian peninsula. *Sci. Nat.* **2021**, *108*, 40. [CrossRef]

88. Di Stefano, G.; Pandolfi, L.; Petronio, C.; Salari, L. The morphometry and the occurrence of *Cervus elaphus* (Mammalia, *Cervidae*) from the Late Pleistocene of the Italian Peninsula. *Riv. It. Paleont. Strat.* **2015**, *121*, 103–120.

89. Pandolfi, L.; Maiorino, L.; Sansalone, G. Did the Late Pleistocene climatic changes influence evolutionary trends in body size of the red deer? The study case of the Italian Peninsula. *Palaeogr. Palaeoclim. Palaeoecol.* **2015**, *440*, 110–115. [CrossRef]

90. Marra, F.; Pandolfi, L.; Petronio, C.; Di Stefano, G.; Gaeta, M.; Salari, L. Reassessing the sedimentary deposits and vertebrate assemblages from Ponte Galeria area (Rome, central Italy): An archive for the Middle Pleistocene faunas of Europe. *Earth-Sci. Rev.* **2014**, *139*, 104–122. [CrossRef]

91. Breda, M.; Lister, A.M. *Dama roberti*, a new species of deer from the early Middle Pleistocene of Europe, and the origins of modern fallow deer. *Quat. Sci. Rev.* **2013**, *69*, 155–167. [CrossRef]

92. Gliozzi, E.; Abbazzi, L.; Ambrosetti, P.G.; Argenti, P.; Azzaroli, A.; Caloi, L.; Capasso Barbato, L.; Di Stefano, G.; Ficcarelli, G.; Kotsakis, T.; et al. Biochronology of selected mammals, molluscs and ostracods from the Middle Pliocene to the Late Pleistocene in Italy. The state of the art. *Riv. It. Paleont. Strat.* **1997**, *103*, 369–388.

93. Palombo, M.R. Twenty years later: Reflections on the Aurelian European land mammal age. *Alp. Mediterr. Quat.* **2018**, *31*, 177–180.

94. Mecozzi, B.; Sardella, R.; Breda, M. Late Early to late Middle Pleistocene medium-sized deer from the Italian Peninsula: Implications for taxonomy and biochronology. *Palaeobio. Palaeoenv.* **2024**, *104*, 191–215. [CrossRef]

95. Di Stefano, G.; Petronio, C. Origin and evolution of the European fallow deer (*Dama*, Pleistocene). *N. Jah. Geol. Paläontol. Abh.* **1997**, *203*, 57–75. [CrossRef]

96. Pandolfi, L.; Petronio, C.; Salari, L. Catastrophic death assemblages from the Late Pleistocene of Italy: The case of Avetrana Karst filling (Taranto, Douthern Italy). *Riv. It. Paleont. Strat.* **2013**, *119*, 109–124.

97. Tong, H.W.; Chen, X.; Zhang, B.; Wang, F.G. New fossils of *Bos primigenius* (Artiodactyla, Mammalia) frm Nihewan and Longhua of Hubei, China. *Vertebr. PalAs.* **2018**, *56*, 69–92.

98. Maniakas, I. Contribution to the Study of Chrono-Spatial Distribution of Palaeocological Adaptations of European Pleistocene Bovini Based on Ecomorphological Analyses and Geometric Morphometrics. Ph.D. Thesis, Aristotle University of Thessaloniki, Thessaloniki, Greece, 2019.

99. Brugal, J.P. Le *Bos primigenius* Boj., 1827 du Pléistocène moyen des grottes de Lunel-Viel (Hérault). *Bull. Mus. d'Anthropol. Préhistor. Monaco* **1985**, *28*, 7–62.

100. Cassoli, P.F.; Di Stefano, G.; Tagliacozzo, A. I vertebrati dei livelli superiori (A e Alfa) della serie stratigrafica di Notarchirico. In *Notarchirico Un Sito Del Pleistocene Medio-Iniziale Nel Bacino di Venosa (Basilicata)*; Piperno, M., Ed.; Edizione Osanna: Venosa, Italy, 1999; Volume 1, pp. 361–438.

101. Pereira, A.; Nomade, S.; Voinchet, P.; Bahain, J.J.; Falguères, C.; Garon, H.; Lefèvre, D.; Raynal, J.P.; Scao, V.; Piperno, M. The earliest securely dated hominin fossil in Italy and evidence of Acheulian occupation during glacial MIS 16 at Notarchirico (Venosa, Basilicata, Italy). *J. Quat. Sci.* **2015**, *30*, 639–650. [CrossRef]

102. Martínez-Navarro, B.; Rook, L.; Papini, M.; Libsekal, Y. A new species of bull from the Early Pleistocene paleoanthropological site of Buia (Eritrea): Parallelism on the dispersal of the genus *Bos* and the Acheulian culture. *Quat. Int.* **2010**, *212*, 169–175. [CrossRef]

103. Martínez-Navarro, B.; Karoui-Yaakoub, N.; Oms, O.; Amri, L.; López-García, J.M.; Zerai, K.; Blain, H.-A.; Mtimet, M.-S.; Espigares, M.-P.; Ben Haj Ali, N.; et al. The early Middle Pleistocene archeopaleontological site of Wadi Sarrat (Tunisia) and the earliest record of *Bos primigenius*. *Quat. Sci. Rev.* **2014**, *90*, 37–46. [CrossRef]

104. Martínez-Navarro, B.; Rabinovich, R. The fossil Bovidae (Artiodactyla, Mammalia) from Gesher Benot Ya'aqov, Israel: Out of Africa during the Early–Middle Pleistocene transition. *J. Hum. Evol.* **2011**, *60*, 375–386. [CrossRef] [PubMed]

105. Martínez-Navarro, B.; Pérez-Carlos, J.A.; Palombo, M.R.; Rook, L.; Palmqvist, P. The Olduvai buffalo *Pelorovis* and the origin of *Bos*. *Quat. Res.* **2007**, *68*, 220–226. [CrossRef]

106. Milli, S.; Palombo, M.R.; Patera, A.; Moscatelli, M.; Anzidei, A.P.; Cazzella, G. New elephant remains in the early Middle Pleistocene of the Roman basin (Latium, Italy): Taphonomy, sedimentology, and GIS methodology. *Mammoth Site Sci. Pap.* **2005**, *4*, 114–119.

107. Marra, F.; Nomade, S.; Pereira, A.; Petronio, C.; Salari, L.; Sottili, G.; Bahain, J.-J.; Boschian, G.; Di Stefano, G.; Falguères, F.; et al. A review of the geologic sections and the faunal assemblages of Aurelian Mammal Age of Latium (Italy) in the light of a new chronostratigraphic framework. *Quat. Sci. Rev.* **2018**, *181*, 173–199. [CrossRef]

108. Iurino, D.A.; Mecozzi, B.; Iannucci, A.; Moscarella, A.; Strani, F.; Bona, F.; Gaeta, M.; Sardella, R. A Middle Pleistocene wolf from central Italy provides insights on the first occurrence of *Canis lupus* in Europe. *Sci. Rep.* **2022**, *12*, 2882. [CrossRef]

109. Alhaique, F.; Argento, A.; di Sassoferrato, B.C.D.A.; Caricola, I.; Fiore, I.; Giaccio, B.; Lemorini, C.; Mazzini, I.; Mercurio, S.; Monaco, L.; et al. From preventive archaeology to valorization and dissemination, with the contribution of scientific investigations. Preliminary data on the MIS 11c (415–406 ka) site of via del Casale Lumbroso (Massimina, Rome, Italy). *BPI* 2024, *in press*.

110. Villa, P.; Boschian, G.; Pollarolo, L.; Saccà, D.; Marra, F.; Nomade, S.; Pereira, A. Elephant bones for the Middle Pleistocene toolmaker. *PloS ONE* **2021**, *16*, e0256090. [CrossRef]

111. Marra, F.; Pereira, A.; Boschian, G.; Nomade, S. MIS 13 and MIS 11 aggradational successions of the Paleo-Tiber delta: Geochronological constraints to sea-level fluctuations and to the Acheulean sites of Castel di Guido and Malagrotta (Rome, Italy). *Quat. Int.* **2022**, *616*, 1–11. [CrossRef]

112. Mecozzi, B.; Iurino, D.A.; Profico, A.; Rosa, C.; Sardella, R. The wolf from the Middle Pleistocene site of Ostiense (Rome): The last occurrence of *Canis mosbachensis* (Canidae, Mammalia) in Italy. *Hist. Biol.* **2021**, *33*, 2031–2042. [CrossRef]

113. Pereira, A.; Nomade, S.; Moncel, M.H.; Voinchet, P.; Bahain, J.J.; Biddittu, I.; Falguères, C.; Giaccio, B.; Manzi, G.; Parenti, F.; et al. Integrated geochronology of Acheulian sites from the southern Latium (central Italy): Insights on human-environment interaction and the technological innovations during the MIS 11-MIS 10 period. *Quat. Sci. Rev.* **2018**, *187*, 112–129. [CrossRef]

114. Peretto, C.; Arzarello, M.; Bahain, J.J.; Boulbes, N.; Douville, E.; Falguères, C.; Frank, N.; Garcia, T.; Lembo, G.; Moigne, A.M.; et al. Guado San Nicola (Monteroduni, Prov. di Isernia). *Not. Preist. Protostoria* **2014**, *1*, 3–5.

115. Pereira, A.; Nomade, S.; Shao, Q.; Bahain, J.J.; Arzarello, M.; Douville, E.; Falguères, C.; Frank, N.; Garcia, T.; Lembo, G.; et al. 40Ar/39Ar and ESR/U-series dates for Guado San Nicola, Middle Pleistocene key site at the Lower/Middle Palaeolithic transition in Italy. *Quat. Geochron.* **2016**, *36*, 67–75. [CrossRef]

116. Biddittu, I. (Ed.) *Guida Del Museo Preistorico di Pofi Frosinone*; Tipografia Nuova Stampa: Frosinone, Italy, 2004.

117. Nomade, S.; Muttoni, G.; Guillou, H.; Robin, E.; Scardia, G. First 40Ar/39Ar age of the Ceprano man (central Italy). *Quat. Geochron.* **2011**, *6*, 453–457. [CrossRef]

118. Panarello, A.; Palombo, M.R.; Biddittu, I.; Mietto, P. Fifteen years along the "Devil's Trails": New data and perspectives. *Alp. Mediterr. Quat.* **2017**, *30*, 137–154.

119. Conato, V.; Esu, D.; Malatesta, A.; Zarlenga, F. New data on the Pleistocene of Rome. *Quaternaria* **1980**, *22*, 131–176.

120. Caloi, L.; Palombo, M.R.; Zarlenga, F. Late-Middle Pleistocene mammal faunas of Latium (central Italy): Stratigraphy and environment. *Quat. Int.* **1998**, *47*, 77–86. [CrossRef]

121. Anzidei, A.P.; Bulgarelli, G.M.; Catalano, P.; Cerilli, E.; Gallotti, R.; Lemorini, C.; Milli, S.; Palombo, M.R.; Pantano, W.; Santucci, E. Ongoing research at the late Middle Pleistocene site of La Polledrara di Cecanibbio (central Italy), with emphasis on human–elephant relationships. *Quat. Int.* **2022**, *255*, 171–187. [CrossRef]

122. Palombo, M.R.; Milli, S.; Rosa, C. Remarks on the biochronology of the late Middle Pleistocene mammalian faunal complexes of the Campagna Romana (Latium, Italy). *Geol. Romana* **2004**, *371*, 135–143.

123. Marra, F.; Ceruleo, P.; Pandolfi, L.; Petronio, C.; Rolfo, M.F.; Salari, L. The aggradational successions of the Aniene River Valley in Rome: Age constraints to early Neanderthal presence in Europe. *PloS ONE* **2017**, *12*, e0170434. [CrossRef]

124. Rosa, C. The Casal de' Pazzi site in the light of new geological and geomorphological data. *J. Mediterr. Earth Sci.* **2023**, *15*, 69–79.

125. Palombo, M.R.; Magri, D.; Molinaro, A.; Pisano, V. The Pleistocene sequence of Campo del Conte (Lower Sacco Valley, Southern Lazio). *Geol. Romana* **2002**, *36*, 289–309.

126. Mancini, M.; Marini, M.; Moscatelli, M.; Stigliano, F.; Cavinato, G.P.; Di Salvo, C.; Simionato, M. Stratigraphy of the Palatine Hill (Rome, Italy): A record of repeated MiddlePleistocene-Holocene paleovalley incision and infill. *Alp. Mediterr. Quat.* **2018**, *31*, 171–194.

127. De Angelis D'Ossat, G. Geologia del Colle Palatino in Roma. *Mem. Descr. Carta Geol. d'It.* **1956**, *32*, 4–95.

128. Pereira, A.; Monaco, L.; Marra, F.; Nomade, S.; Gaeta, M.; Leicher, N.; Palladino, D.M.; Sottili, G.; Guillou, H.; Scao, V.; et al. Tephrochronology of the central Mediterranean MIS 11c interglacial (~425–395 ka): New constraints from the Vico volcano and Tiber delta, central Italy. *Quat. Sci. Rev.* **2020**, *243*, 106470. [CrossRef]

129. Cioni, R.; Sbrana, A.; Bertagnini, A.; Buonasorte, G.; Landi, P.; Rossi, U.; Salvati, L. Tephrostratigraphic correlations in the Vulsini, Vico and Sabatini volcanic succession. *Period. Mineral.* **1997**, *56*, 137–155.

130. Marra, F.; Rohling, E.J.; Florindo, F.; Jicha, B.; Nomade, S.; Pereira, A.; Renne, P.R. Independent ^{40}Ar/^{39}Ar and ^{14}C age constraints on the last five glacial terminations from the aggradational successions of the Tiber River, Rome (Italy). *Earth Planet Sci. Lett.* **2016**, *449*, 105e117. [CrossRef]

131. Giaccio, B.; Marino, G.; Marra, F.; Monaco, L.; Pereira, A.; Zanchetta, G.; Gaeta, M.; Leicher, N.; Nomade, S.; Palladino, D.M.; et al. Tephrochronological constraints on the timing and nature of sea-level change prior to and during glacial termination V. *Quat. Sci. Rev.* **2021**, *263*, 106976. [CrossRef]

132. Lisiecki, L.E.; Raymo, M.E. A Pliocene-Pleistocene stack of 57 globally distributed benthic d18O records. *Paleoceanography* **2005**, *20*, PA1003.

133. Tzedakis, P.C.; Hodell, D.A.; Nehrbass-Ahles, C.; Mitsui, T.; Wolff, E.W. Marine isotope stage 11c: An unusual interglacial. *Quat. Sci. Rev.* **2022**, *284*, 107493. [CrossRef]

134. Hu, H.M.; Marino, G.; Pérez-Mejías, C.; Spötl, C.; Yokoyama, Y.; Yu, J.; Rohling, E.; Kano, A.; Ludwig, P.; Pinto, J.G.; et al. Sustained North Atlantic warming drove anomalously intense MIS 11c interglacial. *Nat. Commun.* **2024**, *15*, 5933. [CrossRef] [PubMed]

135. Tzedakis, P.C.; Drysdale, R.N.; Margari, V.; Skinner, L.C.; Menviel, L.; Rhodes, R.H.; Taschetto, A.S.; Hodell, D.A.; Crowhurst, S.J.; Hellstrom, J.C.; et al. Enhanced climate instability in the North Atlantic and southern Europe during the Last Interglacial. *Nat. Commun.* **2018**, *9*, 4235. [CrossRef] [PubMed]

136. Tzedakis, P.C. Towards an understanding of the response of southern European vegetation to orbital and suborbital climate variability. *Quat. Sci. Rev.* **2005**, *24*, 1585–1599. [CrossRef]

137. CombourieuNebout, N.; Bertini, A.; RussoErmolli, E.; Peyron, O.; Klotz, S.; Montade, V.; Fauquette, S.; Allen, J.; Fusco, F.; Goring, S.; et al. changes in the central Mediterranean and Italian vegetation dynamics since the Pliocene. *Rev. Palaeobot. Palynol.* **2015**, *218*, 127147.

138. Kousis, I.; Koutsodendris, A.; Peyron, O.; Leicher, N.; Francke, A.; Wagner, B.; Giaccio, B.; Knipping, M.; Pross, J. Centennial-scale vegetation dynamics and climate variability in SE Europe during Marine Isotope Stage 11 based on a pollen record from Lake Ohrid. *Quat. Sci. Rev.* **2018**, *190*, 20–38. [CrossRef]

139. Oliveira, D.; Desprat, S.; Yin, Q.; Naughton, F.; Trigo, R.; Rodrigues, T.; Abrantes, F.; SanchezGoñi, M.F. Unraveling the forcings controlling the vegetation and climate of the best orbital analogues for the present interglacial in SW Europe. *Clim. Dyn.* **2018**, *51*, 667–686. [CrossRef]

140. Moncel, M.H.; Arzarello, M.; Peretto, C. The hoslteinian period in Europe (MIS 11–19). *Quat. Int.* **2016**, *409*, 1–270. [CrossRef]

141. Marinelli, F.; Moncel, M.; Lemorini, C. The use of bones as tools in Late Lower Paleolithic of Central Italy. *Sci. Rep.* **2024**, *14*, 11666. [CrossRef]

142. Ashton, N.; Lewis, S.G.; Parfitt, S.; White, M. Riparian landscapes and human habitat preferences during the Hoxnian (MIS 11) Interglacial. *J. Quat. Sci.* **2006**, *21*, 497505. [CrossRef]

143. Ashton, N.; Lewis, S.G.; Parfitt, S.; Penkman, K.E.; Coope, G.R. New evidence for complex climate change in MIS 11 from Hoxne, Suffolk, UK. *Quat. Sci. Rev.* **2008**, *27*, 652668. [CrossRef]

144. Kahlke, R.D.; García, N.; Kostopoulos, D.S.; Lacombat, F.; Lister, A.M.; Mazza, P.P.A.; Spassov, N.; Titov, V.V. Western Palaearctic palaeoenvironmental conditions during the Early and early Middle Pleistocene inferred from large mammal communities, and implications for hominin dispersal in Europe. *Quat. Sci. Rev.* **2011**, *30*, 1368–1395. [CrossRef]

145. Polly, P.D.; Eronen, J.T. Mammal associations in the Pleistocene of Britain: Implications of ecological niche modelling and a method for reconstructing palaeoclimate. In *The Ancient Human Occupation of Britain*; Ashton, N., Lewis, S.G., Stringer, G., Eds.; Developments in Quaternary Sciences; Elsevier: Amsterdam, The Netherlands, 2011; Volume 1, pp. 279–304.

146. Candy, I.; Schreve, D.C.; Sherriff, J.; Tye, G.J. Marine Isotope Stage 11: Palaeoclimates, palaeoenvironments and its role as an analogue for the current interglacial. *Earth-Sci. Rev.* **2019**, *128*, 1851. [CrossRef]

147. Palombo, M.R. Faunal dynamics in SW Europe during the late Early Pleistocene: Palaeobiogeographical insights and biochronological issues. *C. R. Palevol* **2018**, *17*, 247261. [CrossRef]

148. Blain, H.A.; Lozano-Fernández, I.; Ollé, A.; Rodríguez, J.; Santonja, M.; PérezGonzález, A. The continental record of Marine Isotope Stage 11 (Middle Pleistocene) on the Iberian Peninsula characterized by herpetofaunal assemblages. *J. Quat. Sci.* **2015**, *30*, 667–678. [CrossRef]
149. Limondin-Lozouet, N.; Antoine, P.; Bahain, J.-J.; Cliquet, D.; Coutard, S.; Dabkowski, J.; Falguères, C.; Ghaleb, B.; Locht, J.-L.; Nicoud, E.; et al. North-West European MIS 11 malacological successions: A framework for the timing of Acheulean settlements. *J. Quat. Sci.* **2015**, *30*, 702–712. [CrossRef]
150. Monaco, L.; Palladino, D.M.; Gaeta, M.; Marra, F.; Sottili, G.; Leicher, N.; Mannella, G.; Nomade, S.; Pereira, A.; Regattieri, E.; et al. Mediterranean tephrostratigraphy and peri-Tyrrhenian explosive activity revaluated in light of the 430–365 ka record from Fucino Basin (central Italy). *Earth Sci. Rev.* **2021**, *220*, 103706. [CrossRef]
151. Giaccio, B.; Leicher, N.; Mannella, G.; Monaco, L.; Regattieri, E.; Wagner, B.; Zanchetta, G.; Gaeta, M.; Marra, F.; Nomade, S.; et al. Extending the tephra and palaeoenvironmental record of the Central Mediterranean back to 430 ka: A new core from Fucino Basin, central Italy. *Quat. Sci. Rev.* **2019**, *225*, 106003. [CrossRef]
152. Mannella, G.; Giaccio, B.; Zanchetta, G.; Regattieri, E.; Niespolo, E.M.; Pereira, A.; Renne, P.R.; Nomade, S.; Leicher, N.; Perchiazzi, N.; et al. Palaeoenvironmental and palaeohydrological variability of mountain areas in the central Mediterranean region: A 190 ka-long chronicle from the independently dated Fucino palaeolake record (central Italy). *Quat. Sci. Rev.* **2019**, *210*, 190–210. [CrossRef]
153. Grant, K.M.; Rohling, E.J.; Ramsey, C.B.; Cheng, H.; Edwards, R.L.; Florindo, F.; Heslop, D.; Marra, F.; Roberts, A.P.; Tamisiea, M.E.; et al. Sea-level variability over five glacial cycles. *Nat. Commun.* **2014**, *5*, 5076. [CrossRef]
154. Mancini, M.; Moscatelli, M.; Stigliano, F.; Cavinato, G.P.; Marini, M.; Pagliaroli, A.; Simionato, M. Fluvial facies and stratigraphic architecture of Middle Pleistocene incised valleys from the subsoil of Rome (Italy). *J. Mediterr. Earth Sci. Spec. Issue* **2013**, *89*, 93.
155. Palombo, M.R.; Panarello, A.; Mietto, P. Did elephants meet humans along the Devil's path? A preliminary report. *Alp. Mediterr. Quat.* **2018**, *31*, 83–87.
156. Palombo, M.R. The Casal de' Pazzi mammalian fauna: Biochronological and paleoecological notes, and research perspectives. *J. Mediterr. Earth Sci.* **2023**, *15*, 18135. [CrossRef]
157. Zarattini, A. (Ed.) Indagine Geoarcheologica e Paleo-Ambientale (Isoletta, Arce). Tethys, Unpublished Report for Vianini SpA. 1999.
158. Corrado, P.; Magri, D. A late Early Pleistocene pollen record from Fontana Ranuccio (central Italy). *J. Quat. Sci.* **2011**, *26*, 335–344. [CrossRef]
159. Margari, V.; Roucoux, K.; Magri, D.; Manzi, G.; Tzedakis, P.C. The MIS 13 interglacial at Ceprano, Italy, in the context of Middle Pleistocene vegetation changes in southern Europe. *Quat. Sci. Rev.* **2018**, *199*, 144–158. [CrossRef]
160. Alberdi, M.T.; Palombo, M.R.; Strani, F.; Bellucci, L. The large horse from Fontana Ranuccio (Anagni Basin, central Italy). *Hist. Biol.* **2023**, 1–17. [CrossRef]
161. Caloi, L. New forms of equids in Western Europe and palaeoenvironmental changes. *Geobios* **1997**, *30*, 267–284. [CrossRef]
162. Mancini, M.; Di Salvo, C.; Giallini, S.; Marini, M.; Simionato, M.; Caciolli, M.C.; Cavinato, G.P.; Moscatelli, M.; Polpetta, F.; Sirianni, P.; et al. The subsoil of the Colosseum and the detection of the ancient Tiber river Paleovalley (MIS 12–11) in Rome. *J. Mediterr. Earth Sci.* **2023**, *15*, 18067. [CrossRef]